ARISTOTLE UNIVERSITY OF THESSALONIKI
SCHOOL OF SCIENCES - DEPARTMENT OF PHYSICS
SECTION OF ASTROPHYSICS, ASTRONOMY & MECHANICS
LABORATORY OF ASTRONOMY

PHOTOMETRIC STUDY AND DETECTION OF PERIODICITIES IN CATACLYSMIC VARIABLE STARS

DIPLOMA THESIS BY
STYLIANOS A. PYRZAS

THESSALONIKI, 2007

To those who stare upwards...

Contents

List of Figures

List of Tables

Abstract

The purpose of this Diploma Thesis is to present an account of, photometrically, observed Cataclysmic Variable stars (CV's). An extended theoretical overview familiarises the reader with these systems. The thesis focuses on observations of two particular CV's: HS2325+8205 and RXJ0636+3535. Information about the targets, the telescope, the instruments used and the observations themselves is provided. An indepth account of the data reduction code and its functions is given. A detailed description of the resulting lightcurves and their further analysis, in order to detect possible periodicities, follows. Finally, the results are put into physical context.

Acknowledgements

You would probably not be reading this diploma thesis if it wasn't for the efforts and goodwill of various people. The least I can do, is acknowledge them here.

First of all, although I'm quite sure he wouldn't wish this, I would like to thank Professor John H. Seiradakis (A.U.Th.) for supervising my thesis, for all his help during the work, his pointfull comments and suggestions, which greatly improved the text you hold. Most of all, I would like to thank him for always being there, throughout the years of my studies.

Professor Stavros I. Avgoloupis (A.U.Th.) is the man responsible for my involvement with Observational Astronomy. For this, I will always be grateful. But that's the least of things. Professor Avgoloupis has been my mentor and guide to all my steps and, in many cases, a good friend.

I do not think that a few lines can account for the invaluable help of Dr Boris Gänsicke (University of Warwick, UK). I want to thank him for getting me involved with Cataclysmic Variables, for supporting my trip to Warwick, where more than half of the thesis was written, for providing the reduction code and for being ready at any time to answer whatever (usually silly ...) questions I had on the subject and on the reduction code.

I would also like to thank Domitilla de Martino (Osservatorio Astronomico di Capodimonte, Istituto Nazionale di Astrofisica, Italy) for the insight she has provided me with on Intermediate Polars.

Special thanks go to Evanggelos Tsorlinis (A.U.Th.) and George Dimou (N.O.A.) for teaching me everything I know about telescopes.

My fellow student Dimitris Mislis has been more than supportive in many of my astronomical endeavours.

I feel deep gratitude for my family, for supporting me in all possible ways, for backing my up on any choice I have or haven't made and for providing everything I ever needed (and not ...)

To all my friends and those I hold dear, thank you for standing by my side.

Finally, I owe much to the late Emilios Harlaftis (N.O.A.), without whom, none of this would have happened. May he rest in peace.

Chapter 1

Cataclysmic Variables

1.1 Introduction

Cataclysmic variables are among the most intriguing objects one can encounter in the Universe, objects that during the last decades undergo extensive research by professional astronomers yielding exciting results.

The reason for this is that, first of all, they are the most variable stars in the sky. Secondly, their class is so diverse - they can vary in a prolific number of ways, both in amplitude and in a variety of timescales, continuously and unpredictably, never exactly repeating themselves - that each new system can bring forward a new feature and either complicate things a lot more or really help us understand them! Third, when studying cataclysmic variables one often comes across accretion discs and the process of accretion in general. This is a process with fundamental meaning in Astrophysics, as it can be found in star forming regions (and it is from those accretion discs that planets may form as well), in the environment of black holes, in the centre of AGN's and in quasars and so on. But young stars are usually surrounded by dust clouds and our view is obscured, black holes can only be detected in indirect ways and AGN's and quasars are so far away, that only a limited amount of useful information about accretion can be obtained. However, this does not apply on cataclysmic variables, and their study can give us a unique view and understanding of these processes.

In this first chapter of the diploma thesis, the theory behind cataclysmic variables is presented. We analyse the components of a cataclysmic variable and introduce the physics that drives certain processes, such as mass transfer, accretion disc formation, radiation emission etc. Finally, a short overview of the evolution of such systems is given.

1.2 Terminology - Definitions

Cataclysmic Variable Stars or Cataclysmic Variables - CV's, in the astronomical jargon - are semi-detached, interacting binary systems, consisting, mainly, of a white dwarf (WD) and, usually, a low mass main sequence star, an M dwarf (dM). For better understanding, this description will be fully analysed in Sections 1.3 and 1.4.

There are many ways to classify CV's, but usually this is done by taking into account the magnetic field of the white dwarf. Table 1.2.1 presents one such CV classification.

Non-magnetic CV's	**Magnetic CV's**
novalike variables	intermediate polars
dwarf novae	polars

Table 1.2.1: CV magnetic field division.

Before we deal with the physics of CV's and their components, it would be helpful if we put things into context and give the necessary, and widely used, terminology for cataclysmic variables as well as binary stars in general:

- **Binary system**
  Two stars, gravitationally bound to each other, orbiting around the common mass centre.

- **Binary components**
  A term referring to the two stars, which the system consists of, as well as any other system related 'object', e.g. an accretion disc.

- **Primary star**
  The brighter star of the binary system. Everything that has to do with the primary star is denoted with the number 1, eg $M_1, R_1, T_{\rm eff,1}$ are the mass, the radius and the effective temperature of the primary star respectively.

- **Secondary star**
  The fainter star of the binary system. Everything that has to do with the secondary star is denoted with the number 2, eg $M_2, R_2, T_{\rm eff,2}$ are the mass, the radius and the effective temperature of the secondary star respectively.

- **Binary separation**
  The distance of the two stars or - to be more exact - the distance of the centres of mass of the stars.

- **Absolute orbit**
  The orbit of the stars with reference to the mass centre.

- **Relative orbit**
  The orbit of the secondary star with reference to the primary.

- **Inclination Angle**
  The inclination angle i is the angle under which we are observing the binary system and is defined by the perpendicular, to the orbital plane, line and the line of sight. When the inclination angle is $i = 90°$ we see the system edge-on, while when it is $i = 0°$ we see it face-on.

- **Orbital phase**
  In order to have a better overview of the system, especially of the relative orbit, one can introduce the orbital phase, a number varying from 0 to 1, depicting the positions of the two stars relative to the observer. The standard convention is that the system is in phase 0 when the white dwarf is furthest away from us and in phase 0.5 when it is nearest. The phase is defined modulo 1 - so orbital phases 1, 2, 3 etc show the same position of the binary components.

1.3 Components of a CV

It is time to take a closer look at the composition of cataclysmic variables the white- and the main sequence red dwarf.

1.3.1 The white dwarf

The primary star of a cataclysmic variable is a white dwarf. White dwarfs are stellar "corpses", one of the final stages of stellar evolution. They usually originate from a main sequence star with low or medium mass $M \leq 5M_{\odot}$. More than 90% of the stars belong to this category and should eventually evolve into white dwarfs.

The physics behind the formation of white dwarfs is not the subject of this dissertation. Suffice to say, that a white dwarf is actually the core of the original star, consisting mainly of either helium or carbon/oxygen, the "ashes" of hydrogen fusion, that kept the star in equilibrium - balancing gravity pressure with radiation pressure - during its time in the main sequence.

As the star undergoes the phase of red giant, the weight of the surrounding layers that the core "feels" is extremely large. As a result, the core material gets crushed in a density of about one million times greater than that of Earth. The outer layers - which have expanded to a large distance as they do not feel the gravitational pull of the original core - form a planetary nebula. The hot, dense core gets exposed and can be recognised as a white dwarf. In white dwarfs, it is the Fermi-pressure of the degenerate (a result of the very high density) electrons that balances gravity. It should also be mentioned that white dwarfs possess little or no atmosphere.

As a result of this process, a white dwarf is quite small in dimensions, $R_{\mathrm{WD}} \sim 10^4$ km, and quite dense, $\rho_{\mathrm{WD}} \sim 10^6$ gr/cm^3. Its central temperature is $T_{\mathrm{WD,C}} \sim 10^6 - 10^7$ K, while that of the outtermost layers is significantly lower $T_{\mathrm{WD,EFF}} \sim 10^4 - 10^5$ K. Almost all the white dwarfs have a mass that lies in the region of $0.3M_{\odot} \leq M_{\mathrm{WD}} \leq 1.3M_{\odot}$, with a mean value of about $M_{\mathrm{WD}} \sim 0.5 - 0.7M_{\odot}$. What is very interesting, is that no white dwarf can have a mass $M_{\mathrm{WD}} \geq 1.4M_{\odot}$, the so called *Chandrasekhar limit*.

1.3.2 The red dwarf

A red dwarf is, usually, the secondary star of a cataclysmic variable. Red dwarfs are as small as a main-sequence star can be, occupying the lower right part of the main sequence in the H-R diagram and, all in all, not very impressive. However, the red dwarf is nonetheless the key player in the evolution of the cataclysmic variable, driven by the need to fill its Roche lobe. The red dwarf is also denoted as the mass donor star. It is its mass that forms and shapes the accretion disc. As a consequence of all this, the red dwarf is *tidally locked*, meaning its spin period equals its orbital period.

Regarding the physical parameters of the red dwarf, its dimensions are somewhere in the region of $7 \cdot 10^4 \leq R^1{}_{\mathrm{dM}} \leq 4 \cdot 10^5$, while its effective temperature varies between 3100 K $\leq T_{\mathrm{dM,EFF}} \leq$ 3900 K. Red dwarfs have a mass of $0.1M_{\odot} \leq M_{\mathrm{dM}} \leq 0.5M_{\odot}$.

1.4 Mass transfer

As one slowly begins to dive into the physics of cataclysmic variables, mass transfer is the first thing one comes across. It is exactly the procedure of mass transfer that defines the class of cataclysmic variables. In this section we will deal with questions such as *"Why does mass transfer occur?"* and *"What is the binary's response to it?"*.

[1] So a red dwarf - although the smallest star - is still much larger than a white dwarf

1.4.1 The Roche Geometry

In order to understand when mass transfer is possible, one needs to examine the binary system from a dynamical point of view. For that, we need the Roche geometry and, in particular, the Roche lobes shapes (eg [4], [6]). It is the state of the secondary star inside its Roche lobe that defines the behaviour and the evolution of the binary system, so it is usefull and necessary to examine the Roche lobes carefully.

The total gravitational potential of a binary system in a point defined by a vector $\vec{r}$, consisting of stars with masses M_1 and M_2, located at distances $\vec{r}_1$ and $\vec{r}_2$ respectively, consists of three terms: two terms giving the potentials of the two stars and a term due to the centrifugal force related to the angular frequency of the orbit $\vec{\omega}$. Thus, we have

$$\Phi = -\frac{GM_1}{|\vec{r} - \vec{r}_1|} - \frac{GM_2}{|\vec{r} - \vec{r}_2|} - \frac{1}{2}\left(\vec{\omega} \times \vec{r}\right) \tag{1.4.1}$$

In the analysis above we have assumed two things: first, that tidal forces have coerced the two stars into a circular orbit and second, that the mass of each star is concentrated in its centre.

Using equation 1.4.1, for a variety of Φ values, we can draw specific surfaces called *equipotential surfaces*, which means surfaces where Φ is constant. Such an example is given in Figure (1.4.1).

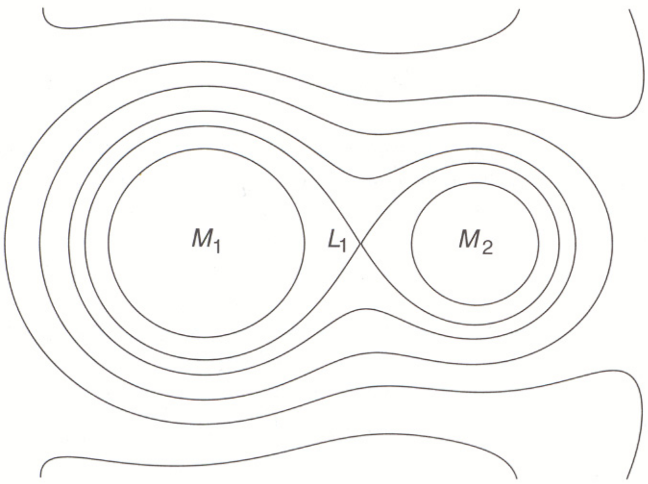

Figure 1.4.1: The equipotential surfaces of a binary system. Figure taken from [1]

As we can see, the equipotential surfaces near the centres of the star are circular, while the ones in scales comparable to the binary separation are pear-shaped. We can also see that, for a specific value of Φ the equipotentials touch in a single point, called the *inner Lagrangian point* L_1. The critical surface where the two equipotentials touch is called the *Roche lobe*.

The `shape` of the Roche lobes is determined by the, so called, *mass ratio* q, defined by $q = M_2/M_1$ and the `scale` of the lobes is set by the binary separation. Two very usefull equations for a binary system with separation equal to α are the ones giving the distance of the point L_1 from the primary (equation 1.4.2) and the radius of the secondary's Roche lobe[2] (equation 1.4.3).

$$R_{1,L_1} = \alpha\,(0.5 - 0.227log\ q) \qquad 0.1 \leq q \leq 10 \tag{1.4.2}$$

$$R_{2,L_1} = \frac{\alpha 0.49 q^{2/3}}{0.6q^{2/3} + ln\,(1 + q^{1/3})} \qquad \forall q \tag{1.4.3}$$

Mass transfer is then enabled when the secondary star - the *mass donor* star - overfills its Roche lobe. Material can then be transfered through the point L_1 to the white dwarf. This can be easily understood with the help of the following figure, where one envisions the Roche lobes as gravitational potential wells. What we actually see here is a horizontal cut through the potential along the line connecting both stars.

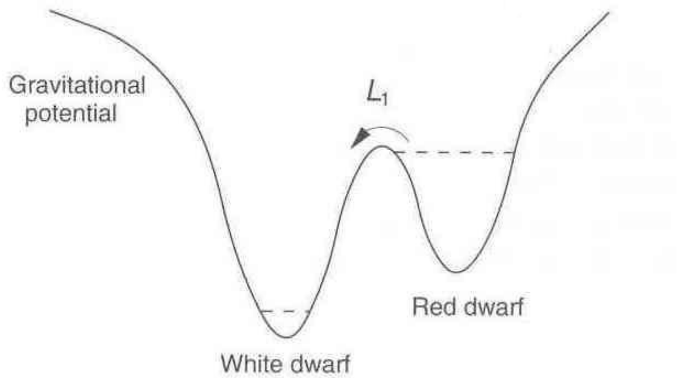

Figure 1.4.2: Gravitational potential wells. Figure taken from [1]

[2]The shape of the Roche lobe is not exactly spherical, because of tidal distortion, so what equation 1.4.3 really gives is the radius of a sphere containing the same volume as the Roche lobe.

Depending on their Roche lobes filling factors, binary stars are divided in the following three categories:

1. *detached:* both stars rest inside their Roche lobes
2. *semi-detached:* one of the stars (over)fills its Roche lobe
3. *contact:* both stars (over)fill their Roche lobes

Categories 2 and 3 are also denoted as *interacting binary systems.*

As we have mentioned before cataclysmic variables are semi-detached systems since the secondary overfills its Roche lobe, enabling mass transfer through the Lagrangian point L_1.

1.4.2 The effects of mass transfer

We will now study the effects of mass transfer on the binary system. An obvious result is that the mass and the radius of the donor star becomes smaller, which also affects the mass ratio q. Furthermore, the orbital period and the binary separation are also affected - although this is not so obvious, at least at first sight - because of the redistribution of angular momentum in the system.

The total angular momentum J is

$$J = \left(M_1 a_1^2 + M_2 a_2^2\right) \omega \tag{1.4.4}$$

where

$$\omega = \frac{2\pi}{P_{\rm orb}} \tag{1.4.5}$$

and

$$a_{\rm i} = \left(\frac{M_{\rm i}}{M}\right) a \qquad i = 1,2 \tag{1.4.6}$$

the distance of the centre of the star from the mass centre, and of course $M = M_1 + M_2$.

Combining the above equations with Kepler's law

$$P_{\rm orb}^2 = \frac{4\pi^2 r^3}{GM} \tag{1.4.7}$$

yields for the total angular momentum

$$J = M_1 M_2 \left(\frac{Ga}{M}\right)^{1/2} \tag{1.4.8}$$

With the - safe - assumption that there are no mass losses, i.e. all the mass from the donor star ends up to the white dwarf, we have $\dot{M} = \dot{M}_1 + \dot{M}_2 = 0$ and $\dot{M}_2 < 0$. Differentiating equation (1.4.8) logarithmically gives

$$\frac{\dot{a}}{a} = \frac{2\dot{J}}{J} - \frac{2\dot{M}_2}{M_2}\left(1 - \frac{M_2}{M_1}\right) \tag{1.4.9}$$

If we suppose that we have conservative mass transfer, meaning $\dot{J} = 0$, then equation (1.4.9) gives a positive $\dot{a}$, because $\dot{M}_2 < 0$ and $M_2 < M_1$ (usually the case in CV's), which means that the binary separation is growing.

With this fact in mind, we are going to examine what happens to the Roche lobe of the secondary. Instead of (1.4.3) we can use the following equation for the radius of the lobe

$$R_{2,\mathrm{L}_1} = a0.462\left(\frac{q}{1+q}\right)^{1/3} \qquad 0.1 < q < 0.8 \tag{1.4.10}$$

Again, differentiating logarithmically yields

$$\frac{\dot{R}_2}{R_2} = \frac{\dot{a}}{a} + \frac{\dot{M}_2}{3M_2} \tag{1.4.11}$$

and using (1.4.9) gives

$$\frac{\dot{R}_2}{R_2} = \frac{2\dot{J}}{J} - \frac{2\dot{M}_2}{M_2}\left(\frac{5}{6} - \frac{M_2}{M_1}\right) \tag{1.4.12}$$

Making the same assumptions as above, and because of the restriction of the values of q in equation (1.4.10), we have $\dot{R}_2 > 0$, so the Roche lobe of the secondary expands.

What do these two conclusions - i.e. $\dot{a} > 0$ and $\dot{R}_2 > 0$ - mean? Simply that, if the secondary does not follow the expansion of the Roche lobe (by expanding itself) mass transfer will stop, as the secondary will not continue to overfill its lobe.

As a conclusion, we can say that, in order to sustain stable mass transfer, the system *must* lose angular momentum, $\dot{J} < 0$. For cataclysmic variables, theory suggests two mechanisms which ensure angular momentum loss (AML): (i) magnetic braking - via a stellar wind - and (ii) gravitational radiation.

A brief discussion about the two mechanisms takes place in (1.8.2). Current knowledge suggests that the former yields a mass transfer rate of $\dot{M} \sim 10^{14}$ kg s^{-1} equivalent to $\sim 10^{-9}$ $M_\odot$ yr^{-1} while the latter a rate of $\dot{M} \sim 10^{13}$ kg s^{-1} equivalent to $\sim 10^{-10}$ $M_\odot$ yr^{-1}.

1.5 The accretion disc

As the red dwarf overfills its Roche lobe, the conditions for mass transfer are fulfilled and matter from the secondary can flow through the Lagrangian point towards the primary. One could perhaps expect that matter would follow a straight line and accrete directly on the white dwarf. This, however, is not the case. What happens instead is that the material follows a trajectory[3], which sweeps past the white dwarf, loops around and intersects itself. This intersection is quite a messy process involving turbulent flows and various viscous phenomena. But, there is one thing we can be sure of, that, eventually, the material will form a ring and settle in a circular orbit around the white dwarf (the lowest energy type of orbit) at a distance called *circularisation radius.*

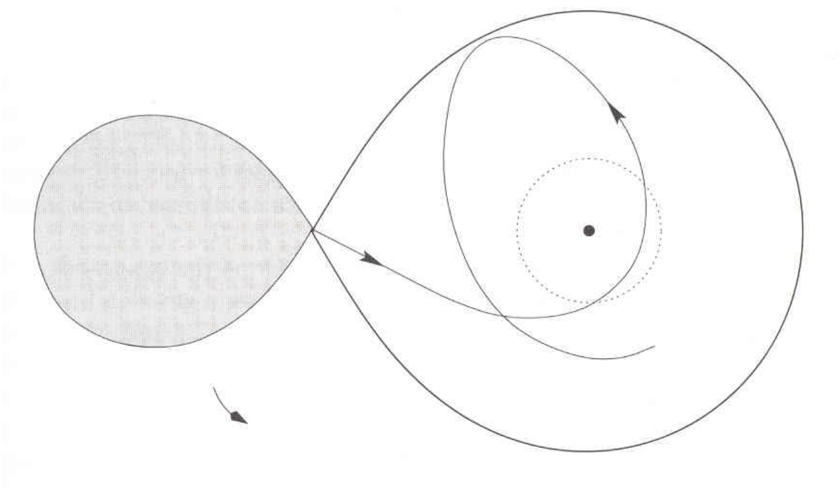

Figure 1.5.1: The trajectory of the mass stream around the white dwarf. Figure taken from [1]

Equating the angular momentum at the point L_1, which is

$$R_{\mathrm{L}_1}\frac{2\pi R_{\mathrm{L}_1}}{P_{\mathrm{orb}}} \tag{1.5.1}$$

with that at the circularisation radius - the dotted line in figure (1.5.1) -

$$r_{\mathrm{circ}}\sqrt{\frac{GM_1}{r_{\mathrm{circ}}}} \tag{1.5.2}$$

[3]To understand a bit more about why this is happening bear in mind that the stream of material is pushed from the stellar wind of the secondary at roughly the speed of sound ~ 10 km s^{-1} through L_1, which, however, orbits perpendicular to this motion at a speed of ~ 100 km s^{-1}

and using Kepler's law (1.4.7), yields for the circularisation radius

$$r_{\mathrm{circ}} = (1+q)\,\frac{R_{\mathrm{L_1}}^4}{a^3} \tag{1.5.3}$$

What happens next is that the ring evolves to form a disc. Disc formation could easily be a dissertation by itself and it is beyond the scopes of this thesis (see for example [2], [3], [22], [23] and [24]).

In general, we can say that material closer to the white dwarf orbits a bit faster[4] and with less angular momentum[5] than adjacent material, which is further out, causing friction, which in turn heats the material and so, energy can be radiated away. This energy is lost to the system (the ring) so, in order for it to be replenished, material moves deeper in the gravitational field.

The role of viscosity is very important in this stage. Because angular momentum needs to be conserved, viscous torques carry angular momentum from the inner to the outer parts. The former will move into even smaller orbits until they accrete directly on the primary, while the latter - gaining angular momentum - will move further out. So, the ring does indeed spread out to form the, so called, *accretion disc.*

The disc is maintained as long as mass transfer continues from the secondary, bringing fresh material and angular momentum.

One could examine the above conclusion mathematically using the following concept: let us assume two test particles with masses m_1, m_2 orbiting the white dwarf at radii r_1, r_2 respectively. The total angular momentum is

$$J = \sqrt{GM_{\mathrm{WD}}}\left(m_1 r_1^{1/2} + m_2 r_2^{1/2}\right) \tag{1.5.4}$$

Differentiating the above equation gives

$$dJ = \frac{\sqrt{GM_{\mathrm{WD}}}}{2}\left(m_1 r_1^{-1/2} dr_1 + m_2 r_2^{-1/2} dr_2\right) \tag{1.5.5}$$

and supposing $dJ = 0$ gives

$$dr_2 = -\frac{m_1}{m_2}\left(\frac{r_2}{r_1}\right)^{1/2} dr_1 \tag{1.5.6}$$

The total energy is

$$E = -\frac{GM_{\mathrm{WD}}}{2}\left(\frac{m_1}{r_1} + \frac{m_2}{r_2}\right) \tag{1.5.7}$$

[4]Bear in mind the Keplerian velocity $v_{\mathrm{kep}} = \sqrt{\frac{GM}{r}}$

[5]The increase in speed is not enough to offset the decrease in radius

which gives

$$dE = \frac{GM_{\rm WD}}{2}\left(\frac{m_1}{r_1^2}dr_1 + \frac{m_2}{r_2^2}dr_2\right) \tag{1.5.8}$$

Equation (1.5.8), using (1.5.6), yields

$$dE = \frac{GM_{\rm WD}m_1 dr_1}{2r_1^2}\left[1 - \left(\frac{r_1}{r_2}\right)^{3/2}\right] \tag{1.5.9}$$

If we examine (1.5.9) for energy loses, $dE < 0$, we see that (i) for $r_1 < r_2$ we have $dr_1 < 0$, which means that the particle orbiting closer to the white dwarf moves inwards, while (ii) for $r_1 > r_2$ we have $dr_1 > 0$, which means that the particle orbiting further from the white dwarf moves outwards.

1.6 Various CV phenomena

In this section we will give a brief account of various phenomena taking place in a cataclysmic variable.

These phenomena contribute to the variability of the CV and, generally, their characteristic signatures can be found in the lightcurves, which will be examined in the next section.

Most of them are periodical, which means they reoccur in specific time intervals. These intervals can be related to the system's *orbital period*, its *orbital phase*, the white dwarf's *spin period* etc

1.6.1 The hot spot

In section (1.5) we have discussed the formation of an accretion disc around the white dwarf, due to mass transfer from the red dwarf, and also that, as long as there are angular momentum losses, mass transfer is maintained.

One can easily understand that, from a particular time point onward, the stream intersects the disc. Radially moving material in the stream meets with disc material circularly orbiting the white dwarf. Due to viscosity and friction, kinetic energy is transformed into heat and is then radiated away, forming an intense *bright* or *hot spot*[6] in the collision area. The hot spot usually contributes a significant amount of the radiation we detect from a cataclysmic variable, as it can be readily observed circling around the primary star.

In some cases, where the width of the stream exceeds the height of the disc, material from the stream can overflow the disc and continue its original,

[6]In this thesis we are going to use both terms

radial, course. This type of accretion is usually denoted as *disc-overflow accretion*.

1.6.2 Orbital humps

Orbital humps are closely related to the hot spot. The orbital hump appears as we see different geometrical projections of the hot spot. We can envision the hot spot orbiting around the white dwarf, to understand that the light we get from the system will vary, because of the appearance or disappearance of the hot spot. This variation can be seen as a periodic, smooth "hump" in a lightcurve, hence the term orbital hump.

1.6.3 Eclipses

The red dwarf, although the smallest star, is still quite larger - by at least an order of magnitude - than the white dwarf. As a result, in systems with high enough inclination, the red dwarf can *eclipse* the white dwarf from the field of view. The red dwarf can also be responsible for the eclipse of the hot spot and also of a part of the accretion disc as well.

Eclipses are very important for the study of cataclysmic variables, as they can give an accurate estimate - if not exact knowledge - of system parameters such as orbital period, red- and white dwarf dimensions etc.

1.6.4 Ellipsoidal modulation

As a result of the massive gravitational pull from the white dwarf, the (initial) spherical shape of the red dwarf becomes distorted, i.e. elongated towards the direction of the white dwarf. Consequently, as the red dwarf orbits around the white one[7], each time it presents a slightly different area - and therefore brightness - to us. This variation in the secondary's brightness is called *ellipsoidal modulation*.

1.6.5 Reflection effects

As mentioned before, the red dwarf is tidally locked in its orbit, which means that it faces the white dwarf always with the same side (similar to the Moon - Earth system).

One can understand that this side - having a really low temperature of $\sim 3000\ K$ - literally gets blasted by the radiation emitted from the ~ 50000

[7]Here we are, of course, referring to the relative orbit. In reality both stars orbit each other around their common mass centre.

K white dwarf! As this side gets heated, it becomes brighter. Again, because of the red dwarf orbiting around the white, we periodically detect an increase of the secondary's brightness, as the hotter side comes in view. This is known as *reflection effect*.

1.6.6 Flickering

If one examines a CV lightcurve carefully (see next section as well), apart from the major periodical variations (eg white dwarf eclipse with the orbital period), one would also distinguish, quite easily in fact, random fluctuations.

These fluctuations are patternless and occur on many different timescales. This effect is called *flickering* and it can be among the strongest characteristics of a CV lightcurve.

Observations show that flickering arises mainly from the inner part of the accretion disc and the hot spot, a process directly related to the turbulent effects taking place in the mass transferring stream.

1.7 Cataclysmic Variable lightcurves

Two are the tools observational astronomers use, when studying cataclysmic variable stars (and, actually, any other kind of objects ...): spectroscopy and photometry.

Photometric observations, ie the study of the system's lightcurve can provide a wealth of important information about the system. We have already mentioned that most of the various CV phenomena presented above can be detected in a lightcurve. It is time we took a closer look to this subject.

1.7.1 Lightcurve features

One of the most prominent features a CV's lightcurve can display is an eclipse. Why does an eclipse have such an effect on the lightcurve? And also, are all eclipse profiles the same?

The answer to the first question is "simple": the eclipse affects the amount of light we detect from the system, thus playing an important role in the shape of the lightcurve.

The answer to the second question is a bit more difficult. Usually, there is a struggle between the white dwarf, the hot spot and the disk itself for light-domination in a CV. Somewhat simplified one can say that the dominant feature will determine the eclipse profile.

For example, let as examine a CV where the white dwarf is dominant. The contribution each star has to the total light we detect from the system is given by the luminosity law. The law

$$L = 4\pi R^2 \sigma T_{\text{eff}}^4 \tag{1.7.1}$$

applied for a white dwarf with $R_1 \sim 10.000$ km and $T_{\text{eff}} \sim 30.000$ K would yield $L_1 \sim 10^{26}$ W, whereas for a red dwarf with $R_2 \sim 100.000$ km and $T_{\text{eff}} \sim 3.000$ K would yield $L_2 \sim 10^{23}$ W.

Clearly, the white dwarf's contribution - in terms of luminosity - dominates by three orders of magnitude. Taking into account Wien's displacement law the maximum flux of the WD comes out in the ultraviolet, so at optical wavelengths the difference may not be three orders of magnitude, but it's still significant. As a result, one expects a quite clear drop in the light we get from the system, once the white dwarf is eclipsed.

Furthermore, since the white dwarf's dimensions are really small, compared to those of the red dwarf, one expects that both the ingress and egress will be very steep.

Another feature of an eclipse in cataclysmic variables is its short duration, compared with the orbital period of the system. This can easily be understood, if one takes into account (i) the small system separation, which is of the order of a couple Solar radii and (ii) the orbital periods, which are of the order of a few hours. These two effects, yield a large relative speed (the speed at which the red dwarf orbits around the white one, for an observer sitting on the white dwarf), which explains the short eclipse duration.

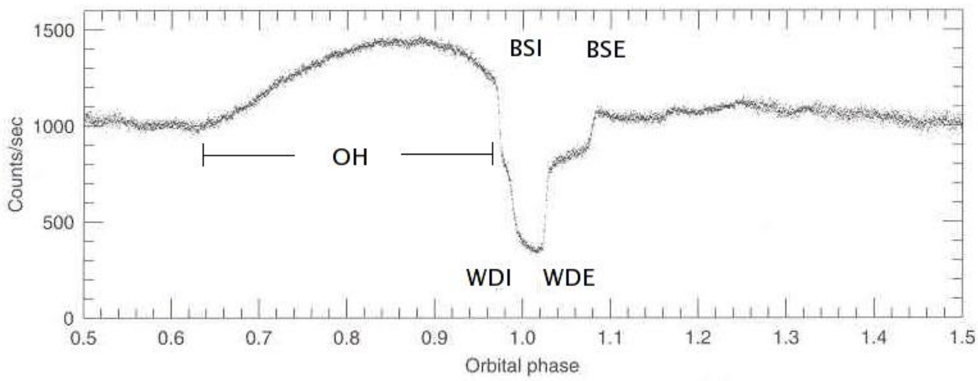

Figure 1.7.1: An example of a CV lightcurve. Figure taken from [1]

An example of a CV lightcurve can be seen in the Figure (1.7.1). The eclipse profile presented above is easily distinguishable. Marked on the figure are the white dwarf ingress [WDI] and egress [WDE] and also the orbital hump [OH] and an eclipse of the bright spot [BSI] and [BSE].

1.8 A brief cv of a CV

As a conclusion to this first, theoretical part of the diploma thesis we will give a brief - and somewhat simplified - curriculum vitae of a Cataclysmic Variable star. In other words, we will deal mainly with the origin of CV's and give some information regarding their evolution .

The subject of CV evolution is one of the hottest research areas in the field. Despite the wealth of observational information on CV's (>600 well studied systems), their formation and evolution is poorly understood. A substantial hurdle in improving the theories of CV evolution is actually the striking lack of knowledge about their progenitors known as pre-CVs, of which currently only ~ 40 are known. But not only the number of known pre-CVs is small, it appears also that these systems are subject to a strong observational selection effect, as most of them contain hot (and therefore still young) white dwarfs. Theoretical work, on the other hand, indicates that the majority of such pre-CV systems should have cooler (older) white dwarfs, something not yet supported by observations.

1.8.1 Forming the WD - dM system

Originally, the binary system comprises of the red dwarf and another, more massive, main sequence star. This star quickly[8] evolves to become a red giant, dramatically increasing its radius. Again, Roche lobes are very important in understanding what happens next.

The red giant overfills its Roche lobe, so material is transfered to the red dwarf. But the angular momentum of the material is increased through the transfer, because it moves away from the common mass centre, which lies nearer to the red giant. In order to conserve the total angular momentum, the binary separation decreases, which results to a decrease in the size of the Roche lobes.

This, in turn, means that the red giant overfills its Roche lobe even more and yet more material is transfered to the red dwarf. The whole process, described above, is repeated and, eventually, the entire envelope of the red giant is dumped onto the companion.

The red dwarf finds itself overwhelmed with all the incoming material and cannot assimilate such influx. Thus, the material forms a cloud surrounding

[8]The lifetime of a star scales as $1/M^2$.

both stars. The binary system enters the, so-called, *common envelope phase.*

Inside the common envelope, the orbital energy of the stars is drained, as they orbit, something that causes them to spiral inwards. To give a quantitative idea of the process and the orders of magnitude of the physical parameters involved, the system separation could decrease from 100 $R_\odot$ to 1 $R_\odot$ in about 1000 years.

1.8.2 Becoming a CV

The two stars, orbiting inside the common envelope, act as a propeller pushing - with a little help from the orbital energy that gets extracted - the envelope away into space, to form a *planetary nebula.* Depending on the separation, the binary is either a new cataclysmic variable or (if the separation is too large for mass transfer to begin) a detached white dwarf - red dwarf binary.

The hallmark of Cataclysmic Variables is mass transfer. As discussed in another part of this thesis, angular momentum loss (AML) from the binary is necessary in order to have a stable mass transfer. Theory suggests this is ensured by two processes: *gravitational radiation* and *magnetic braking.* The former becomes significant in systems with short orbital periods (ie $<$ 2 hrs). The energy to generate the waves is extracted from the binary orbit, which causes inward spiralling. The latter operates through the stellar wind of the red dwarf. Material of the wind follows the lines of the stellar magnetic field, co-rotating with them (of course this is a result of the red dwarfs self-rotation) and getting accelerated. At some point ("breaking point"), they detach from the field lines carrying substantial amounts of angular momentum with them.

1.8.3 CV evolution

Figure (1.8.1) shows the distribution of orbital periods of about 300 cataclysmic variable systems. The orbital period at which a binary becomes a Cataclysmic Variable is determined by the size of the red dwarf when the binary emerges from the common envelope phase. From that point on, as angular momentum loss results in the shrinking of the binary separation, the CV evolves towards shorter orbital periods.

One can have a clearer picture of how this happens through the following example: let us assume a blob of accreting material leaving the red dwarf. The binary expands slightly (trying to conserve angular momentum) and so does the Roche lobe, which detaches from the red dwarf, which shrinks slightly. As AML reduces both the separation and the size of the Roche lobe, contact is resumed at shorter periods, appropriate to the smaller secondary.

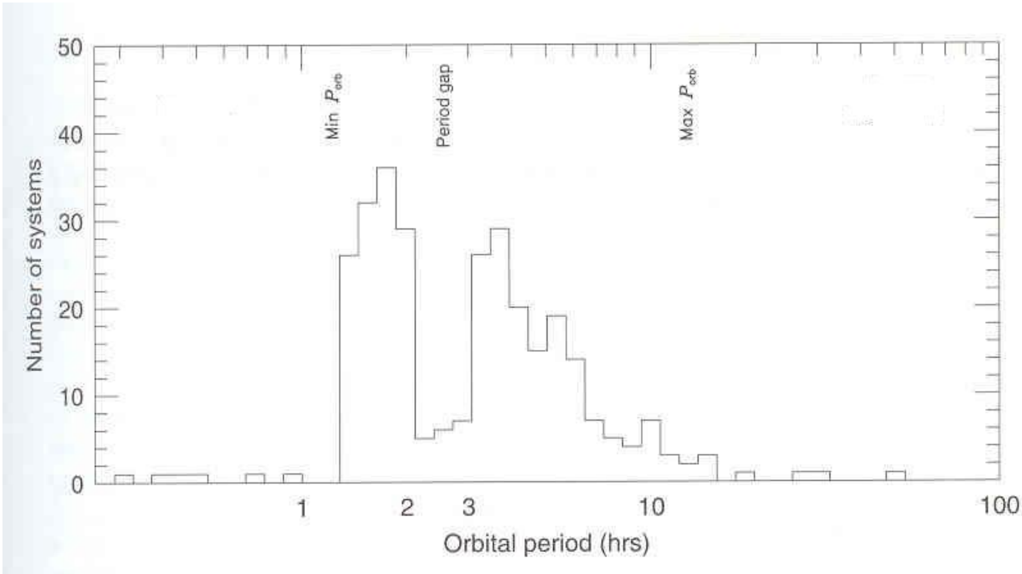

Figure 1.8.1: The distribution of orbital periods of about 300 known cataclysmic variable systems. Figure taken from [1]

There are three, easily distinguishable features in the figure above: first, that only few systems have orbital periods longer than 12 hrs, known as the *long-period cutoff*. Second, that there is an abrupt drop in the number of systems with orbital periods between 2 and 3 hours, referred to as the *period gap*, and third, another sudden cutoff at an orbital period of ~ 78 min, called the *period minimum*.

The long-period cutoff

The long-period cutoff can be explained with the limit that applies to the masses of the binary's stars. The white dwarf's mass cannot exceed the Chandrasekhar limit and the red dwarf cannot be more massive than the white one, in order to avoid rapid mass transfer. The binary separation, and therefore the size of the secondary's Roche lobe, increases with orbital period. A more massive star is needed to fill a larger Roche lobe, so the mass of the star also increases with orbital period. As a result, the limit to the red dwarf's mass leads to a limit on the orbital period of about 12 hrs.

The period gap

The explanation of the period gap is quite more complicated and is beyond the scopes of this thesis. The general concept is that, for systems with orbital periods of 2-3 hrs, mass transfer stops. This occurs because the red dwarf has been driven out of equilibrium, due to the steady mass loss, and it finds itself with too large a radius for its (reduced) mass and so shrinks and detaches from its Roche lobe. Magnetic braking also switches off in this case, so gravitational radiation takes control and slightly reduces the separation until the orbital period drops below 2 hrs and mass transfer is re-established.

The period minimum

The period minimum is also a bit complicated in its explanation. The main idea is that the red dwarf now has such a low mass that it becomes *degenerate*, which means that it now exhibits a peculiar behaviour: its radius response to mass loss is such, that the red dwarf expands! Again, taking the previously mentioned example into mind, we see that the separation expands and the Roche lobe detaches, after a blob of accreting material has left the red dwarf, but now the red dwarf expands slightly as well. So, contact is resumed in slightly longer orbital periods.

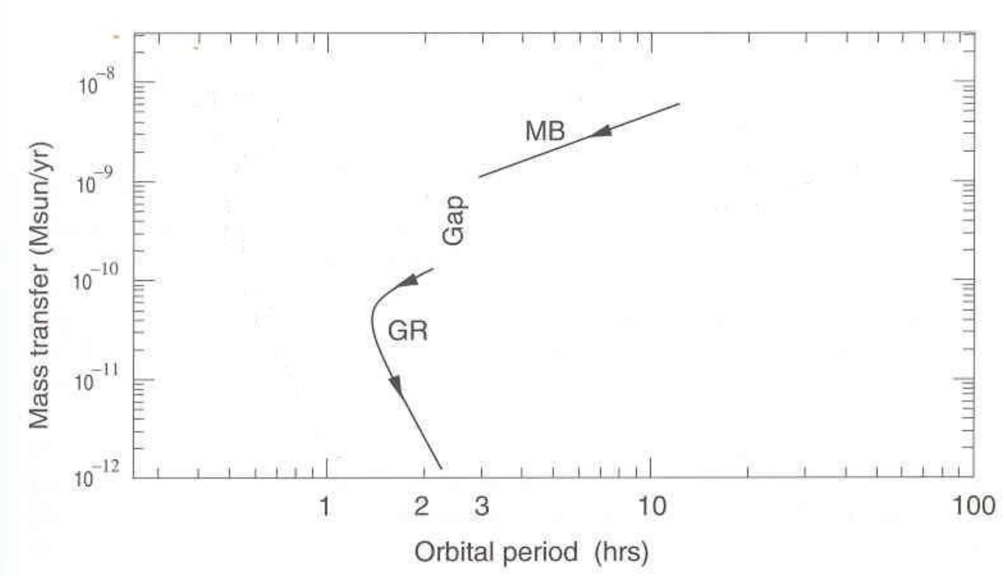

Figure 1.8.2: Evolution of Cataclysmic Variable stars. Figure taken from [1]

The fate of Cataclysmic Variables

Summing up, one can say that, once created, a cataclysmic variable evolves to shorter orbital periods, passes through the period gap, where mass transfer stops and the system is no longer detectable as a CV, resumes mass transfer and continues evolving until the period minimum, where the system “bounces” and starts evolving to longer orbital periods. This can be seen in the Figure (1.8.2).

Where does the evolutionary process stop? After some point, the red dwarf is so low in mass, it actually resembles a Jupiter-like object orbiting the white dwarf. The mass transfer rate is so low, that the binary becomes quite faint and hard to detect.

Having gone over the basic theory of Cataclysmic Variable stars, its time to move to more practical stuff and deal with the observations.

Chapter 2

Observations

2.1 Introduction

In the second chapter of the thesis, a detailed description of the targets observed is presented, along with the complete night log from every observational run. Information about the site, the telescope and the instruments used for the observations is also given.

2.2 The site

Observations took place at the Kryoneri Astronomical Station (KAS) operated by the National Observatory of Athens (NOA, [25]). KAS is located in Korinthia region, Northern Peloponnese, Greece, on the top of mountain Kilini, near a small village, Kryoneri. Table (2.2.1) contains some useful information about the site.

Geogr. Longitude	$22°37'$ E
Geogr. Latitude	$37°58'$ N
Elevation	930 m
Cloudiness statistics (yearly)	45%
Temperature range	$-5°C$ to $+35°C$
Seeing (median)	$1.5''$

Table 2.2.1: Kryoneri Astronomical Station characteristics

2.3 The telescope

The Kryoneri Astronomical Station houses a 1.2m telescope, constructed by Grubb Parsons and installed in 1975. Two different views of the telescope follow (all pictures taken from NOA's website [26]).

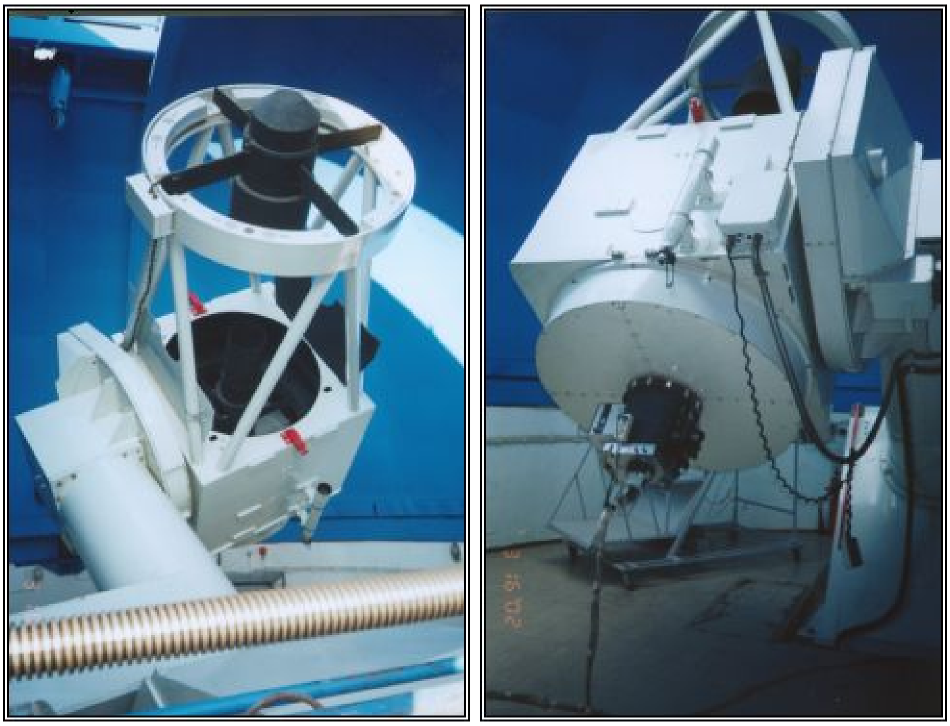

Figure 2.3.1: The 1.2m telescope at Kryoneri Astronomical Station

The main features of the telescope are shown in Table (2.3.1)

Primary mirror	`Type: paraboloidal` `Diameter: 1200mm` `Focal ratio: f/3`
Secondary mirror	`Type: hyperboloidal` `Diameter: 310mm`
Final focal ratio	`f/13`
Focal points	`Cassegrain, Coude`
Field of view	$40'$
Image scale	$12.5''$/mm

Table 2.3.1: The 1.2m telescope characteristics

2.4 The camera

The main scientific instrument of the 1.2m Telescope is a Series 200 CCD Camera System made by Photometrics (now Roper Scientific).

The CCD camera is shown in figure (2.4.1)

Figure 2.4.1: The Series 200 CCD Camera System

The camera characteristics are the following:

CCD type	SI-502, Grade 1, UV-coated
Chip size	516 x 516 pixels
Pixel size	24μ x 24μ
Cooling: Peltier system	up to $-40°$C
Gain	5.17 e^-/ADU (1x gain) 1.23 e^-/ADU (4x gain)
Readout noise	9 e^- RMS (1x gain) 7.5 e^- RMS (4x gain)
Dark current	1.03 e^-/pix/sec

Table 2.4.1: The CCD camera characteristics

In the Cassegrain focus of the telescope, the field size of the CCD is about 2.5 x 2.5 arcmin with pixel size of 0.30 arcsec.

2.5 The targets

The two cataclysmic variable stars presented here were initially observed in research projects the author took part in. As they both exhibit most of the magnificent features of Cataclysmic Variables they were selected for the purposes of this diploma thesis.

2.5.1 HS2325+8205

HS2325+8205 was initially identified as a candidate CV by the Hamburg Quasar Survey [18]. We are still not fully sure as to what kind of (non-magnetic) CV it is. HS2325+8205 exhibits an exciting behaviour, not understood to its full extend (see Chapter 5).

Finding chart

Figure (2.5.1) shows HS2325 finding chart. The star itself is marked with two long straight lines. Comparison star A (see Chapters 3 and 4 for details) is marked with a square, B with a circle and C with two short straight lines. The orientation of the chart is N-up, E-left and the field is $10'$ x $10'$.

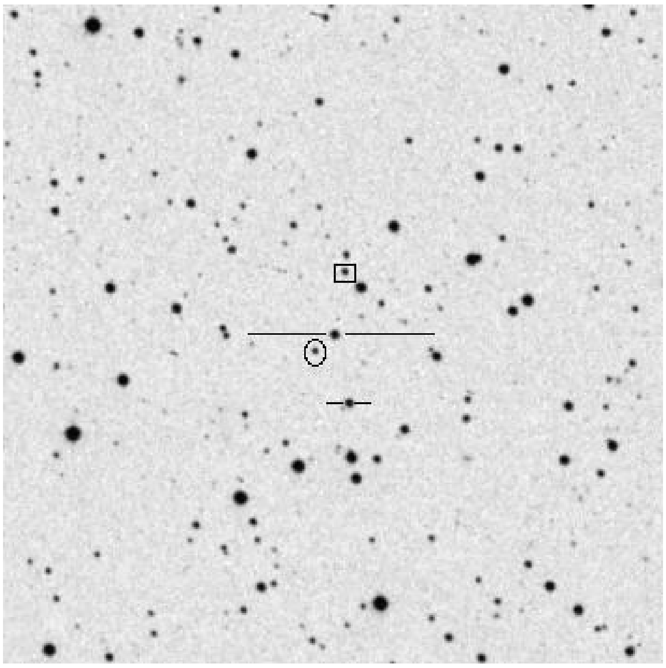

Figure 2.5.1: HS2325+8205 finding chart. The target and the comparison stars are marked.

Basic data

Table (2.5.1) gives the B and R magnitudes as well as the B-R index of HS2325+8205 and the three comparison stars.

Star	*B mag*	*R mag*	*B-R index*
HS2325+8205	15.5	15.4	0.1
Comparison A	16.7	16.3	0.4
Comparison B	17.9	16.5	1.4
Comparison C	15.6	15.2	0.4

Table 2.5.1: The B and R magnitudes and B-R index of HS2325+8205 and comparison stars

Observation log

Table (2.5.2) provides a list of all observing nights for HS2325+8205 along with a variety of information regarding the data gathered.

Date	*Obs Start-End [UT]*	*Filter*	*Exp. Time [sec]*	*Frames #*
05/09/2003	18:09-00:28	clear	30	646
10/06/2004	22:19-23:13	clear	30	090
11/06/2004	21:56-02:15	clear	30	390
12/06/2004	22:50-01:40	clear	30	270
25/07/2004	22:53-02:40	clear	30	389
27/07/2004	19:10-01:44	clear	30	693
21/10/2004	17:05-00:00	clear	20	997
22/10/2004	17:08-23:22	clear	20	897
23/10/2004	17:09-23:05	clear	20	858
23/08/2006	19:42-02:55	clear	30	727
28/10/2006	17:58-22:05	clear	30	595

Table 2.5.2: Observation log of HS2325+8205

2.5.2 RXJ0636+3535

RXJ0636+3535 was initially identified as a bright X-ray source in the ROSAT Bright Source Catalogue [17]. A combined ROSAT/2MASS selection further identified it as a possible CV [8]. In addition to that, we prove that RXJ0636+3535 is an Intermediate Polar (see Chapters 4 and 5 for more details).

Finding chart

Figure (2.5.2) shows RXJ0636 finding chart. The star itself is marked with two long straight lines. Comparison star A is marked with a square, B with a circle and C with two short straight lines. The orientation of the chart is N-up, E-left and the field is $10'$ x $10'$.

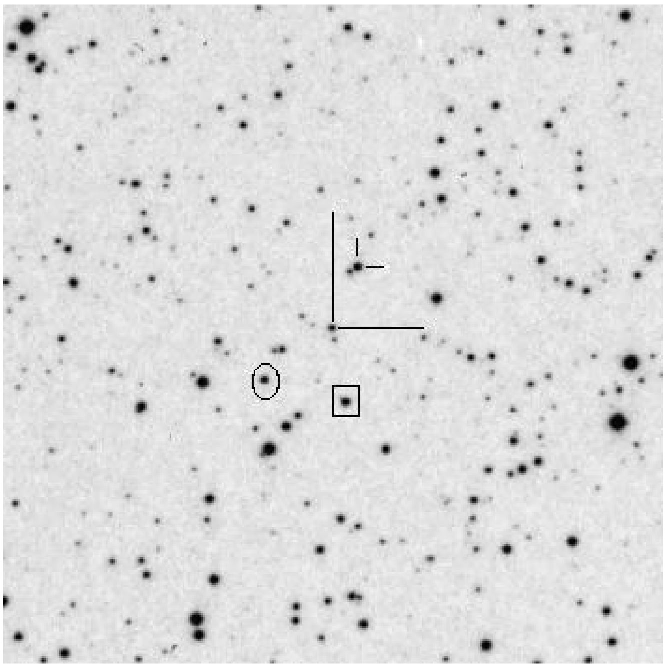

Figure 2.5.2: RXJ0636+3535 finding chart. The target and the comparison stars are marked.

Basic data

Table (2.5.3) gives the same as above basic information for RXJ0636+3535 and its comparisons.

Star	*B mag*	*R mag*	*B-R index*
RXJ0636+3535	15.7	15.9	-0.2
Comparison A	15.7	14.5	1.2
Comparison B	15.7	15.0	0.7
Comparison C	15.3	14.3	1.0

Table 2.5.3: The B and R magnitudes and B-R index of RXJ0636+3535 and comparison stars

Observation log

Table (2.5.2) provides a list of all observing nights for RXJ0636+3535 along with a variety of information regarding the data gathered.

Date	*Obs Start-End [UT]*	*Filter*	*Exp. Time [sec]*	*Frames #*
20/10/2004	01:42-03:33	clear	30	195
21/10/2004	00:07-03:43	clear	20	531
22/10/2004	23:46-03:50	clear	20	492
23/10/2004	23:12-00:37	clear	20	210
21/02/2005	20:46-00:52	clear	45	300
23/02/2005	17:46-01:43	clear	45	600
24/02/2005	17:16-22:17	clear	45	370
03/03/2005	17:55-23:53	clear	45	383

Table 2.5.4: Observation log of RXJ0636+3535

Chapter 3

Data Reduction

3.1 Introduction

A correct reduction procedure of the scientific data is, of course, vital, in order to get a proper lightcurve of the star under study. In this chapter, the data reduction pipeline employed, is presented, along with a description of the reduction procedure.

3.2 The pipeline

The data reduction pipeline was originally written by Dr. Boris Gänsicke, University of Warwick UK (see [19]). It is based on ESO's astronomical software **MIDAS** [26] and on Bertin's **SExtractor** [20].

3.3 The reduction procedure

The pipeline works in four basic steps:

- *Step 1:* Data preparation
- *Step 2:* Star frame calibration
- *Step 3:* Star detection, photometry and frame matching[1]
- *Step 4:* Lightcurve plotting

In the following subsections we will examine each step separately and take a walkthrough of the pipeline functions.

[1]Unfortunately, a necessary procedure, as the tracking of the 1.2m telescope in KAS is sometimes not that accurate

3.3.1 Data preparation

The first thing the pipeline does is to prepare all frames. The frames are first converted from ".fits" format (the format of the CCD Camera in KAS) to ".bdf" - the **MIDAS** compatible format.

After that the frames are trimmed: 5 pixels are removed from every edge to get rid of possible frame-edge-anomalies.

Finally the Julian Date is calculated from the date and UT time of the observations taken from the header of each frame.

3.3.2 Star frame calibration

Raw CCD images cannot readily be reduced, since, besides the useful information, they also contain imperfections created by various factors that influence the quality of the frames. Before one can deal with the useful information and the physics behind it, one needs to get rid of the effects of these factors. For convenience - although not entirely accurate - we will simply refer to these factors as "noise".

There are two main noise factors in each CCD image (*i*) the bias level, which is an instrumental signal offset that should be, in principle, constant over all pixels, but in practice varies over the CCD and (*ii*) the dark current, due to thermal electrons produced by the CCD chip.

One can get an estimate of the bias level through *bias frames*, which are zero-time exposures, or in other words, a simple readout of the unexposed CCD, through the on-chip electronics, through the ADC (Analog-to-Digital Converter), through the cables, to the computer, while *dark frames*, i.e. long (of the order of >30 mins) exposures with, nonetheless, closed shutter, give an estimate of the thermal noise of the camera.

One more thing to take into account is the fact that, theoretically, each pixel should have the same behaviour, meaning that each pixel should give the same amount of electrons for a specific amount of photons. Actually, this is not the case. Because of construction faults, neighbouring pixels can have different sensitivity to the light. As a result, the frame needs to be made homogeneous", normalised, flat in the astronomical jargon.

This is achieved through *flat frames* or *flat fields*, ie uniformly-lit-chip frames. The most common technique for getting flat fields is to point the telescope towards the zenith in the dusk/dawn sky. Flat fields can also help getting rid of dust and stains on the telescope mirror and lenses, the shutter of the CCD or the CCD chip itself.

Noise substraction is the second step in the data reduction pipeline, which makes the following actions:

- Combines all the bias frames to create a *masterbias* frame

- Combines all the dark frames to create a *masterdark* frame

- Combines all the flat frames to create a *masterflat* frame

- Substracts the masterbias and masterdark frame from each and every star frame

- Divides each and every bias and dark subtracted star frame with the masterflat frame

The creation of the master frames is user interactive. This means that the pipeline displays for example each bias frame along with some statistical measurements - such as minimum and maximum counts, mean counts, standard deviation etc - so that the user can decide if a particular bias frame will be used for the creation of the masterbias. The same procedure applies for the dark and flat frames. It should also be noted that the "combination" is achieved by calculating the median of the given frames.

Furthermore, there are some additional internal processes, ie the masterbias gets substracted from each dark frame before the creation of the masterdark and the masterbias and masterdark frames are substracted from each flat frame before the creation of the masterflat.

Our star frames have now been cleaned of the noise and corrected for any other imperfections, so we can begin to deal with the information and the physics contained in them.

3.3.3 Star detection, photometry and frame matching

In order to get the astronomical information out of each frame, one needs to detect the stars in each frame first and, after that, establish how much light each star has contributed in the particular frame. In other words, one needs to perform photometry on each star of the frame.

In order to achieve this, the pipeline uses **SExtractor**, which can both be used for the identification of stars and perform photometry as well. The user modifies two **SExtractor** files called *default.sex* and *default.param* before running the program. The former is the default configuration file of **SExtractor** and contains information about how **SExtractor** should work - e.g. sigma levels, size of the photometric aperture etc - and the latter the kind of output information the user wants - eg X and Y coordinates of stars, fluxes, instrumental magnitudes, errors etc. The resulting output after running **SExtractor** (based on the parameters the pipeline employs) is a file for each frame with 8 columns.

The first column contains the ID number of each star, depending on the sequence of its detection. To make this a bit clearer, let us assume, for example, that **SExtractor** begins "reading" the frame from the upper side to the lower and from the left side to the right. The star which will be detected first will be appointed the ID 1, the second the ID 2 etc.

The second and third columns have the X and Y coordinates of the stars detected.

The fourth and fifth columns contain the (instrumental) magnitudes of the stars and the magnitude error respectively.

The sixth column contains the background value at centroid position, the seventh the FWHM of each star assuming a gaussian core and the eighth the S/G classifier output.

Next in line is frame matching. Although not obvious at first sight, a problem might arise during the star detection step. Previously, we have seen the way **SExtractor** reads a frame and identifies a star, which gets a specific ID number.

Theoretically, if the telescope was guiding and tracking perfectly, the stars would be detected at *exactly* the same position (same pixels) in each frame, so ID 1 in frame 1 and ID 1 in frame 2 would be the *same* star.

However, in reality, the tracking of the 1.2m telescope in the KAS is sometimes not very accurate, and this can cause trouble. Imagine a series of frames. In frame 1, a star is detected first and gets ID 1. As the telescope is not guiding accurately, the field depicted in each frame slowly changes, for example moving downwards. It is quite possible, that another star gets in sight and gets detected first, getting ID 1. So, ID 1 in frame 1 and ID 1 in frame n will *not* correspond to the same star. So, if one tries to plot a lightcurve for star ID 1, the values of the magnitudes from the photometry will be those of different stars.

In order to tackle the problem, one should align the frames. As the procedure of alignment can be somewhat complicated, the pipeline uses the *matching technique* to overcome the difficulties of bad telescope tracking.

This is done by using the astronomical program **MATCH** [27]. How does **MATCH** work? In simple terms, we appoint one frame to be the *reference* frame[2] and **MATCH** calculates the vectors of the stars' relative positions to each other, creating a certain pattern. The program then tries to apply this pattern to all other frames, thus matching the stars in each frame, regardless of their ID number.

[2]This is, usually, the clearest frame, the one with most stars detected

3.3.4 Lightcurve plotting

The final step of the reduction is the plotting of the lightcurve, which is also an interactive procedure.

The pipeline displays the reference frame and asks the user to provide the ID number of the target star. After that it assembles a file containing the Julian Date (from the preparation step), the instrumental magnitude and the magnitude error of the target star from all frames. If, for some reason, the target has not been matched in a number of frames, the pipeline can display these, so that the user can provide the ID number of the target in them, in order for the list to be - fully - completed.

The pipeline employs differential lightcurve plotting. To do that, a comparison star needs to be selected, so that its lightcurve is substracted from the one of the target star.

What exactly is a comparison star? It is a known, strictly[3] *non-variable* star (*standard* stars are usually the best comparisons) used for two main reasons: to get rid of external night variations - eg clouds - and to transform the instrumental magnitude to real. Let us examine these two uses.

It is possible that the target lightcurve displays "fake" variations for example because of clouds in some frames leading to fewer counts. By substracting the lightcurve of the comparison star one can get rid of such variations, since the comparison, in principal, has a straight line lightcurve and the only variations it might exhibit are "fake" ones.

Furthermore, since the comparison has a known real magnitude, the user can easily transform the instrumental magnitude of the target star to real magnitude by taking the instrumental magnitude of the comparison star into account. Of course, this is possible because the CCD Camera in KAS operates linearly.

Exactly same procedure for choosing the target star described above is applied for choosing the comparison star.

The final output of the pipeline is the lightcurve with Julian Date as X-axis and Δmag or real mag as Y-axis - depending if the user has transformed instrumental to real magnitude.

3.4 Further reduction

Getting the lightcurve of a system is only the first step of the data reduction and it usually is quite a straightforward - if not simple - procedure. Proper

[3]Actually... hopefully! That is why it is a good idea to use at least two comparison stars to check if they are constant.

analysis is needed in order to detect the various periodicities a CV might exhibit.

To achieve this, another pipeline called **PERIOD** [29] is employed, a **SuperMongo** [28] interface to the **MIDAS**/TSA context, the Time Series Analysis utility of Schwarzenberg and Czerny.

Again, there are three basic steps:

- Preliminaries

- Pipeline setup

- Actual analysis

3.4.1 Preliminaries

Since we are interested in accurate time series analysis the first thing the user does is run an appropriate script to perform a Heliocentric Julian Date correction to the original Julian Date values of the lightcurve of the star under investigation.

After that, the user prepares - via another script - a file called *obs.lst*. This file contains all the nights for which the user has lightcurves. This file is extremely important as only the lightcurves therein will be analysed.

3.4.2 Pipeline setup

Next, the user has to setup **PERIOD**. There is a number of options to choose, such as (i) nightly mean substraction, ie the substraction of the nightly mean from the lightcurves before the data are combined to get rid of night-to-night variations which may result in low-frequency power (for an explanation of what *power* means in this case, see the next subsection), (ii) total mean substraction, ie substracting the total mean after combining the data - an advantageous choice if the system has a very long period and only parts of the orbit are covered each night - (iii) HJD[0] substraction, ie the substraction of the HJD of the first data point so that it starts from time=0, (iv) smoothing using box car filters to get rid of flickering, (v) fake frequency sets production, (vi) error bars plotting etc.

Having done this, the user combines all available data by running another script. Everything is now ready to procede with the actual analysis.

3.4.3 Actual analysis

Simplifying things a bit, one can say that CV lightcurves can be divided into two main categories: the sinusoidal and the non-sinusoidal ones, with features such as an eclipse.

Depending on the lightcurve a different approach is required for further analysis. The **PERIOD** pipeline tackles this problem with two packages (a) *Period* and (b) *Eclipse*. We will examine both packages separately.

Period package

The *Period* package is addressed to sinusoidal lightcurves. Its puprose is basically to produce *periodograms* such as the ones described by Scargle [21].

What is a periodogram? In plain terms, it is a Fourier transform of the lightcurve, which analyses the lightcurve into a set of sine waves of various frequencies. The *amplitude* of each sine wave reveals how much of that frequency is present in the lightcurve. The *power* of each sine is connected to the amplitude through $A = 2\sqrt{P}$. Either amplitude or power are plotted against frequency to produce a periodogram.

The user first runs a script to prepare the data to be analysed according to the setup of the pipeline, described previously. After that the user defines the frequency range to be sampled, the number of test frequencies to be used and the kind of periodogram wished.

After the periodogram has been calculated the user can fold the data over a specific frequency. This is done interactively, by running an appropriate set of commands which allow the user to pick a specific frequency - usually the one displaying a high peak (= more power) in the periodogram. The pipeline provides information about the exact frequency value, the error of this and the amplitude of the variation.

The package also provides the option for detrending a frequency, ie fitting and substracting a sine wave of specific frequency from the data. This is useful for getting rid of unwanted sinusoidal modulation in the data, or for setting apart overlapping/merged signal clusters.

Eclipse package

Fourier transforms used in the *Period* package do not perform very well in highly non-sinusoidal curves, for example in the cases where the lightcurve displays eclipses. However, accurate eclipse timing can easily provide information for the orbital period of the system and for other periodicities as well.

That is exactly the purpose of the *Eclipse* package, to calculate the time of eclipse centre. The user can do this in two ways.

The first method mirrors the part of the lightcurve displaying the eclipse. The user can shift the mirrored part until the best overlap with the original one is found. Assuming that the parts of the lightcurve around the eclipse centre are symmetric - and in principal they are - the best overlap will accurately provide the time of the eclipse centre.

The second method is practically a polynomial fit on the eclipse. The user interactively marks the region where the polynom should be fitted. The program determines the eclipse centre by the data points used for the polynomial fit.

Using either one of the two methods the user has now a file with all eclipse centre times from the lightcurves. From this, the program can calculate the period of the system, its ephemeris and an O-C diagram to check this ephemeris.

Chapter 4

Results

4.1 Introduction

In Chapter 2 we have presented the two targets observed for this diploma thesis and given a detailed account of the amount of data gathered during each observing night.

In Chapter 3 we have taken a complete walkthrough of the data reduction pipeline, its uses and the output it produces.

In this Chapter we will present the results from the reduction of the data of the two targets.

4.2 Results for HS2325+8205

HS2325+8205 was observed for eleven nights during the years 2003 to 2006 yielding a total of more than 6500 frames.

Figures (4.2.1) to (4.2.4) show the resulting lightcurves from each night. The lightcurves are shown in sets of 3.

Using the Eclipse package we have determined the eclipse centre times from all the lightcurves displaying an eclipse (or more), applying both the mirroring and the polynom fit method. The results are shown in Table (4.2.1).

The analysis of the eclipse centre times shown in Table (4.2.1) yields and orbital period of $P_{\mathrm{orb}} \sim 0.1943$ cpd or more accurately $P_{\mathrm{orb}} \sim 279.841927 \pm 0.000117$ min for HS2325+8205 as shown in Figure (4.2.5).

The ephemeris deduced from the data of Table (4.2.1) is of the form HJD$[\phi = 0]$ = HJD[0] + E $*$ PERIOD and is the following:

$$T_0 = 2452888.425254 \pm 0.000247 + E * 0.1943346715 \pm 0.0000000815 \quad (4.2.1)$$

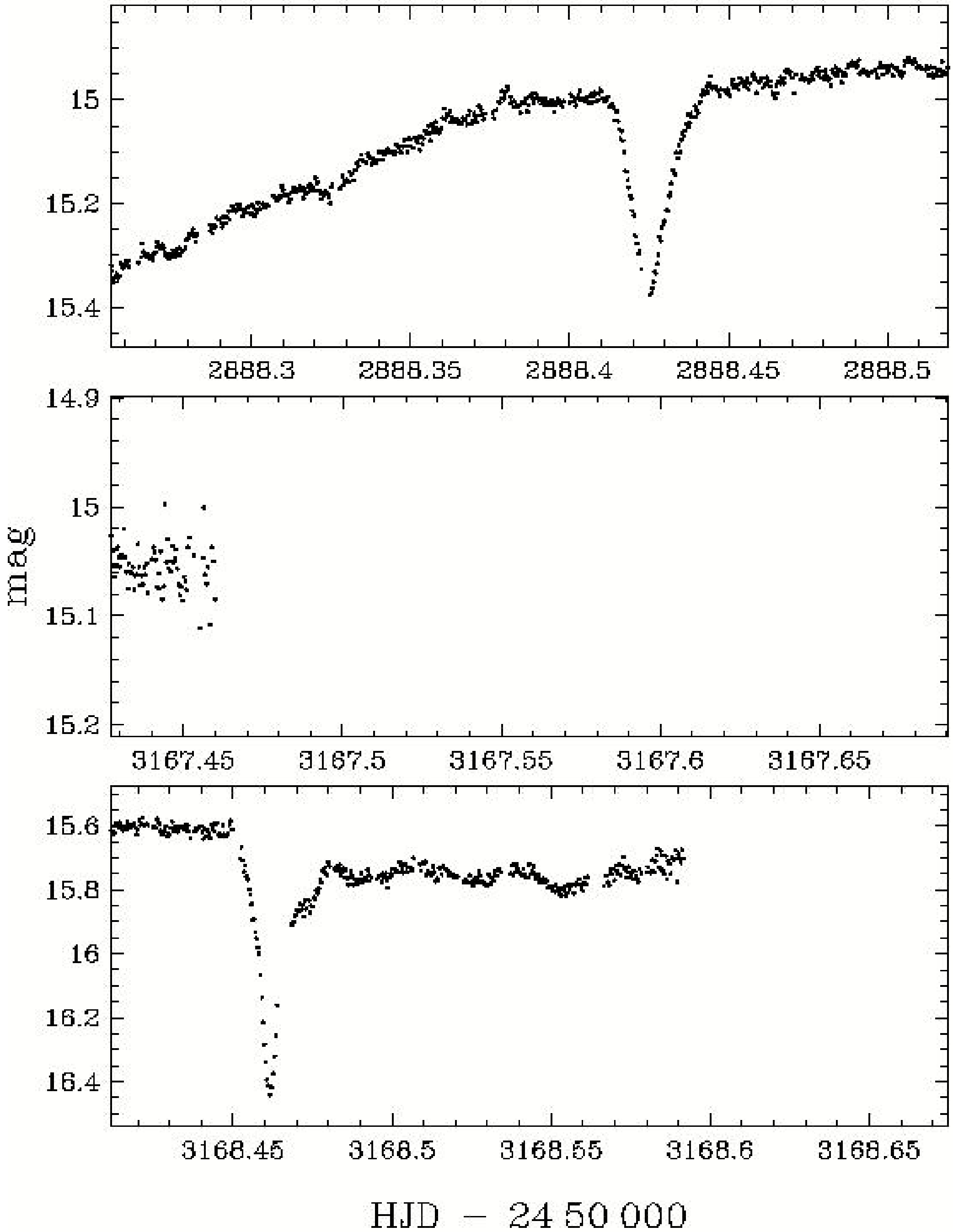

Figure 4.2.1: HS2325+8205 lightcurves. Top to bottom: 05/09/2003, 10/06/2004, 11/06/2004

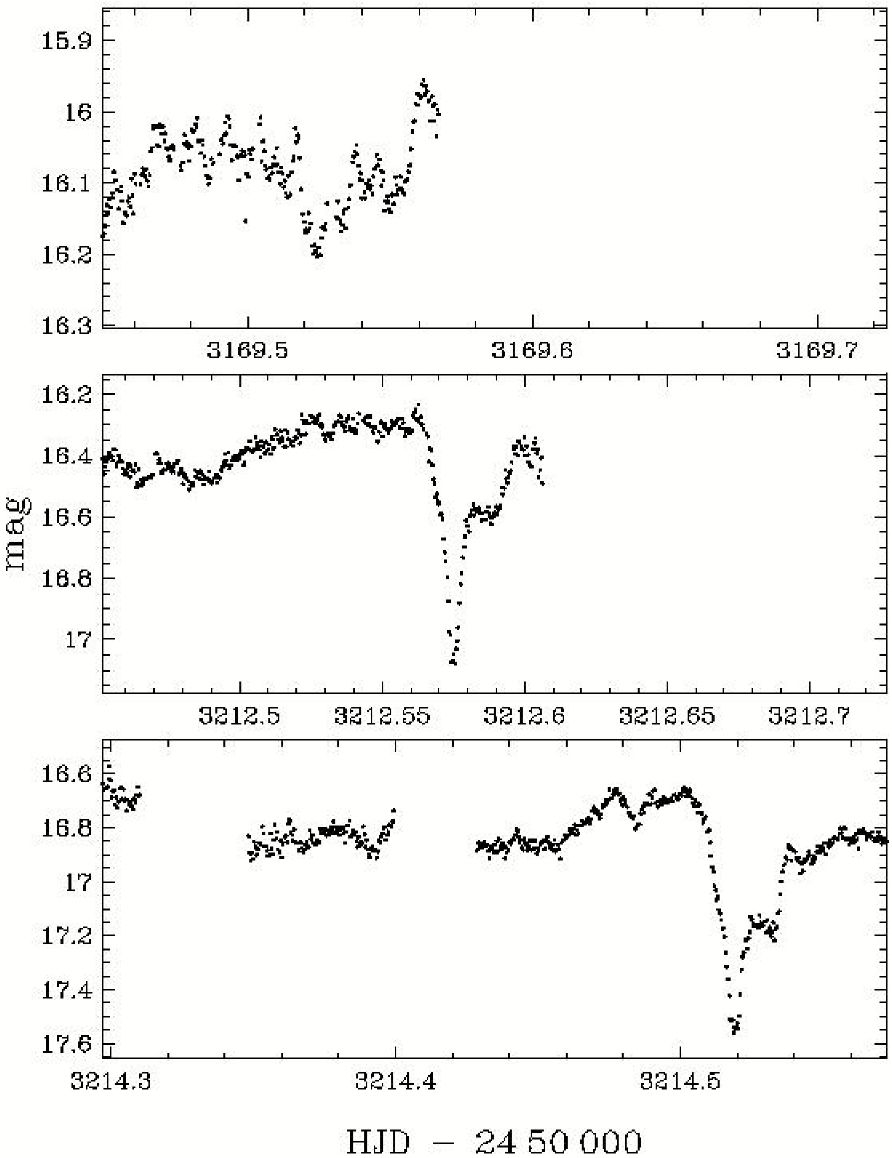

Figure 4.2.2: HS2325+8205 lightcurves. Top to bottom: 12/06/2004, 25/07/2004, 27/07/2004

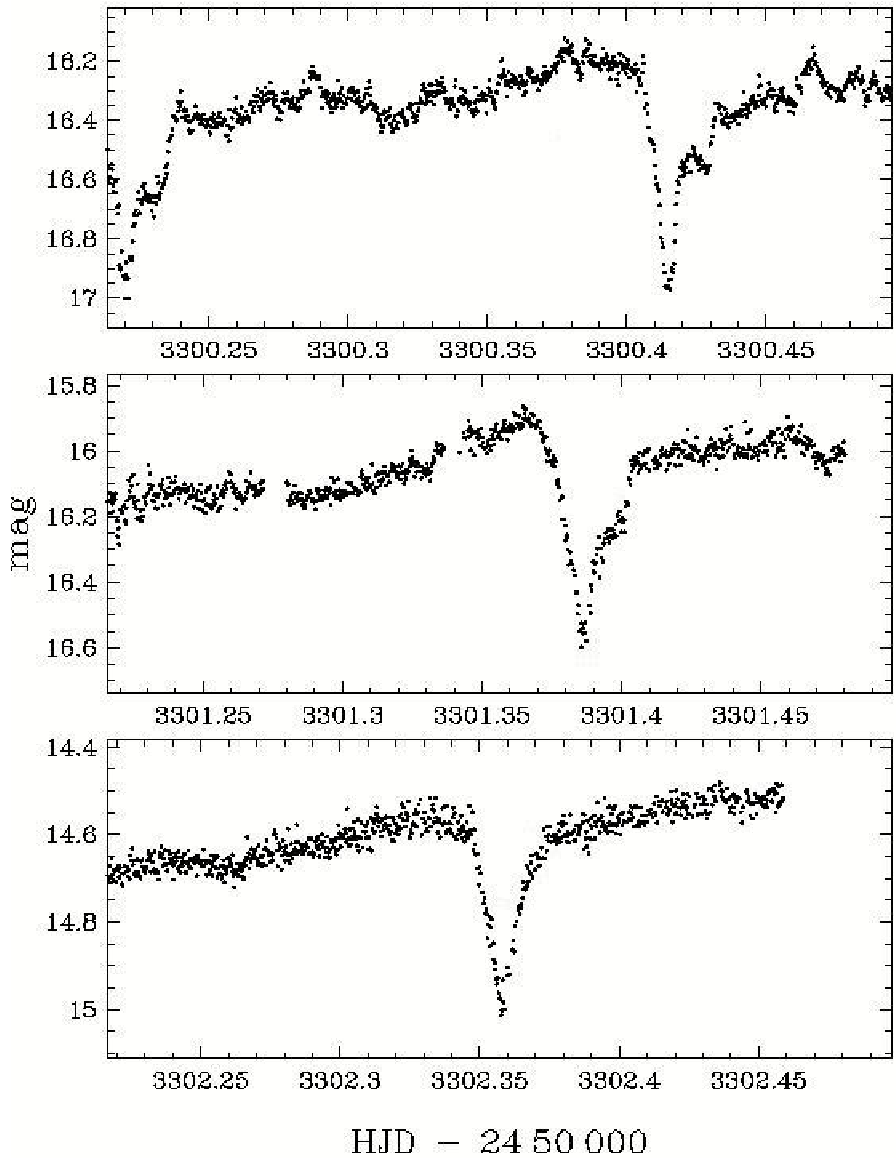

Figure 4.2.3: HS2325+8205 lightcurves. Top to bottom: 21/10/2004, 22/10/2004, 23/10/2004

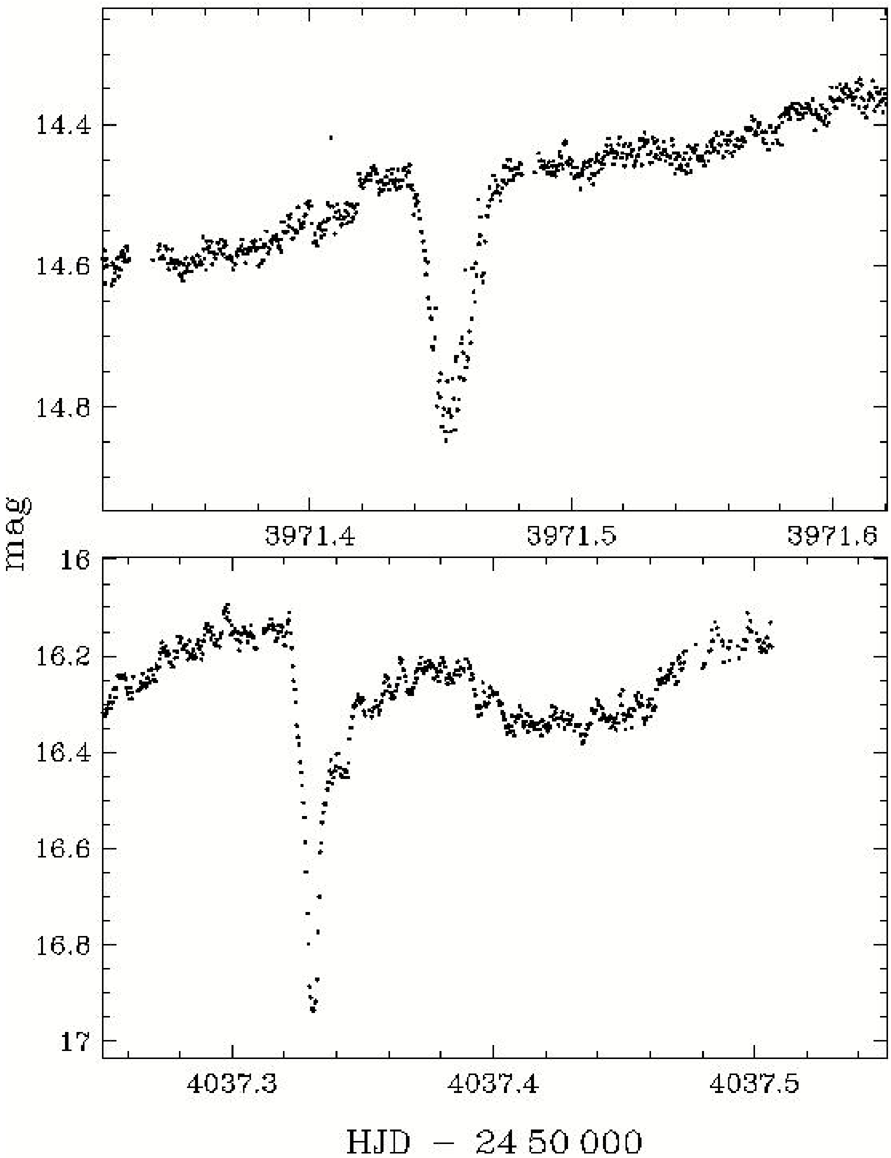

Figure 4.2.4: HS2325+8205 lightcurves. Top to bottom: 23/08/2006, 28/10/2006

Obs. night	*Mirroring times*	*Polynom Fit times*
05/09/2003	2452888.425281	2452888.425249
11/06/2004	2453168.461566	2453168.461618
25/07/2004	2453212.575227	2453212.574946
27/07/2004	2453214.518959	2453214.519344
21/10/2004	2453300.220219	2453300.220552
21/10/2004	2453300.414815	2453300.414449
22/10/2004	2453301.386414	2453301.386836
23/10/2004	2453302.358235	2453302.359029
23/08/2006	2453971.453278	2453971.452549
28/10/2006	2454037.331020	2454037.331141

Table 4.2.1: Eclipse centre times for HS2325+8205

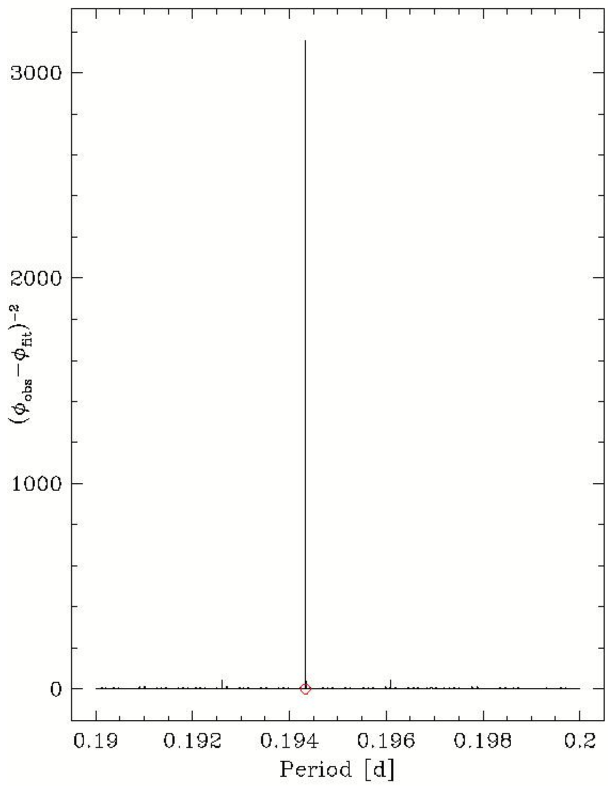

Figure 4.2.5: Orbital period calculation for HS2325+8205

4.3 Results for RXJ0636+3535

RXJ0636+3535 was observed for eight nights during the years 2004 to 2005 yielding a total of more than 3000 frames.

Figures (4.3.2) to (4.3.5) show the resulting lightcurves from each night. The lightcurves are shown in sets of 2.

Using the *Period* package we have calculated a Scargle periodogram from all available lightcurves. The periodogram, shown in Figure (4.3.1) clearly displays two strong clusters of signals at $F_1 \sim 86$ cpd and at $F_2 \sim 93$ cpd , each with 1-d aliases of similar power.

The periodicities corresponding to the peak of each signal cluster are $P_1 = 16.8057 \pm 0.0001$ min and $P_2 = 15.5021 \pm 0.0002$ min respectively.

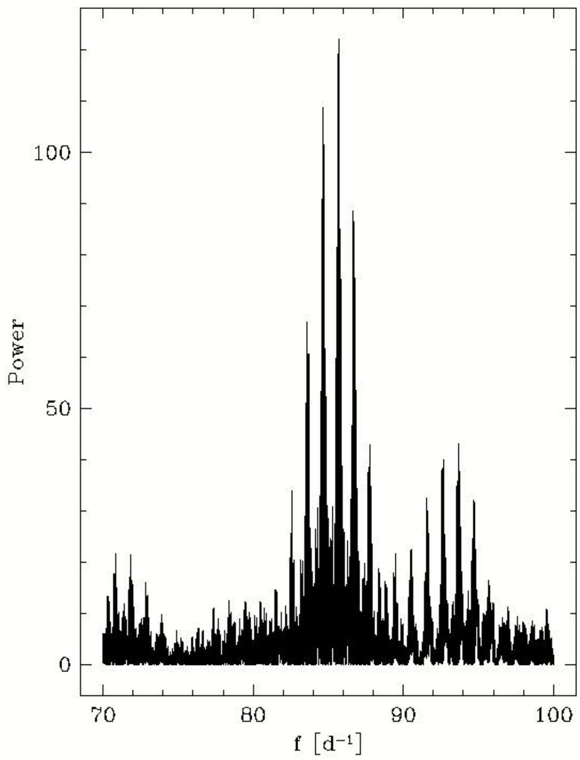

Figure 4.3.1: Scargle periodogram for RXJ0636+3535

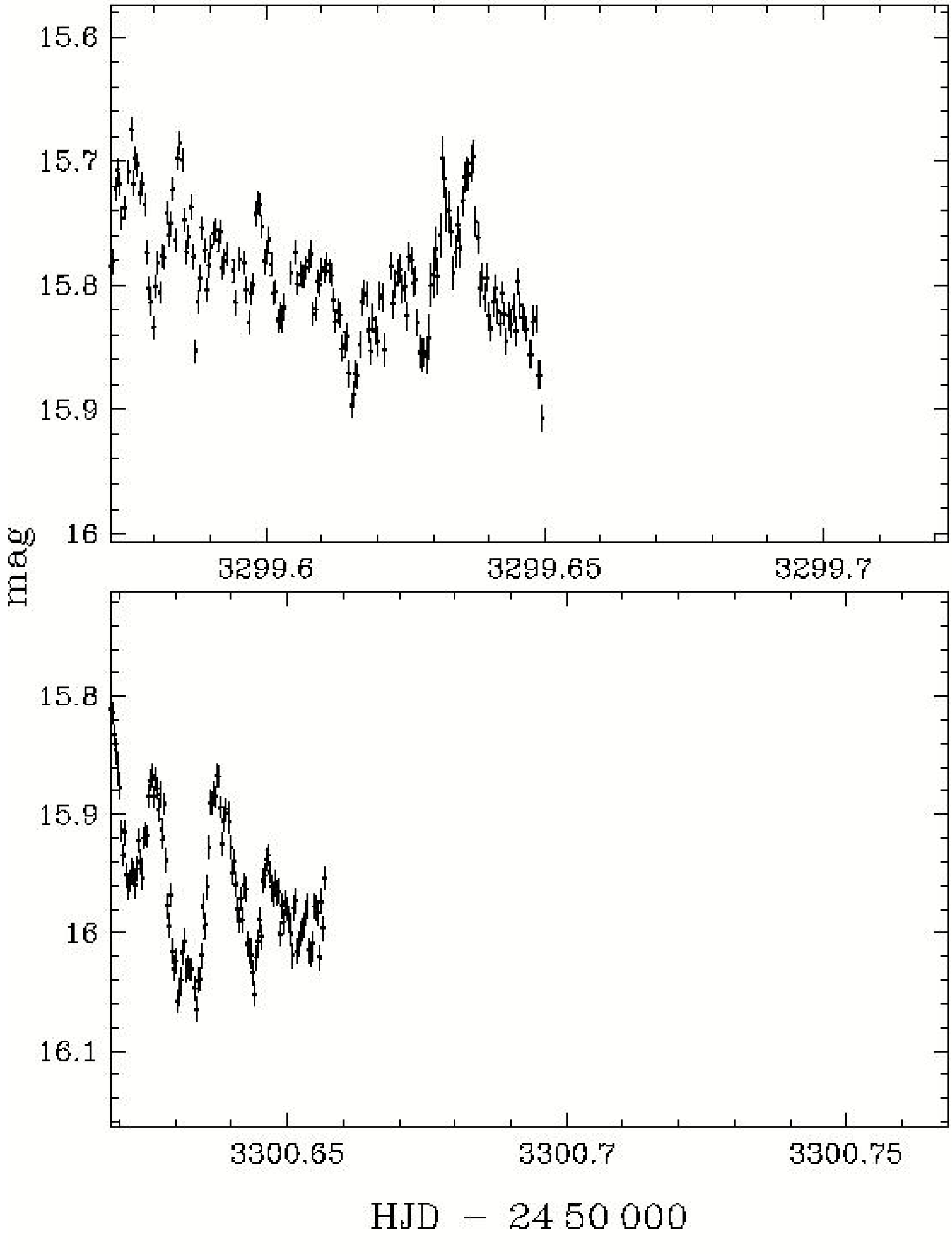

Figure 4.3.2: RXJ0636+3535 lightcurves. Top to bottom: 20/10/2004, 21/10/2004

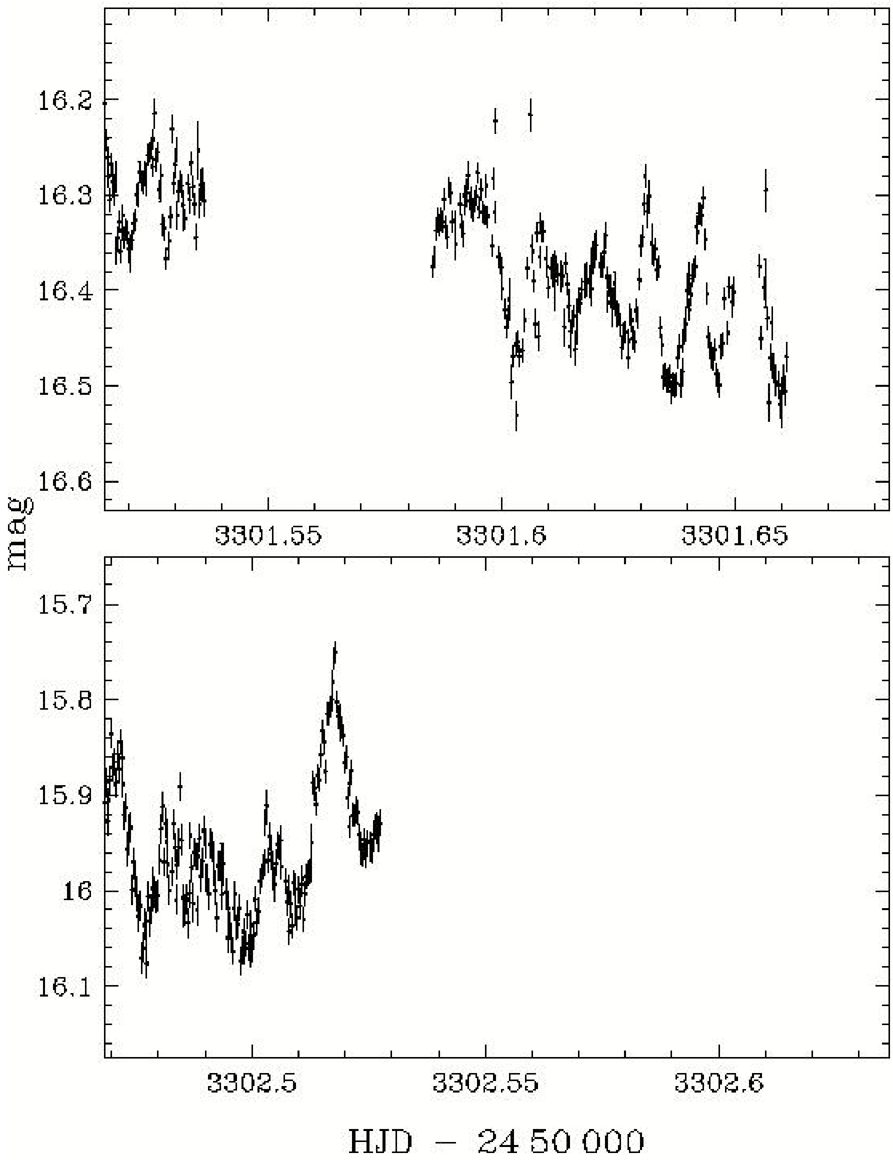

Figure 4.3.3: RXJ0636+3535 lightcurves. Top to bottom: 22/10/2004, 23/10/2004

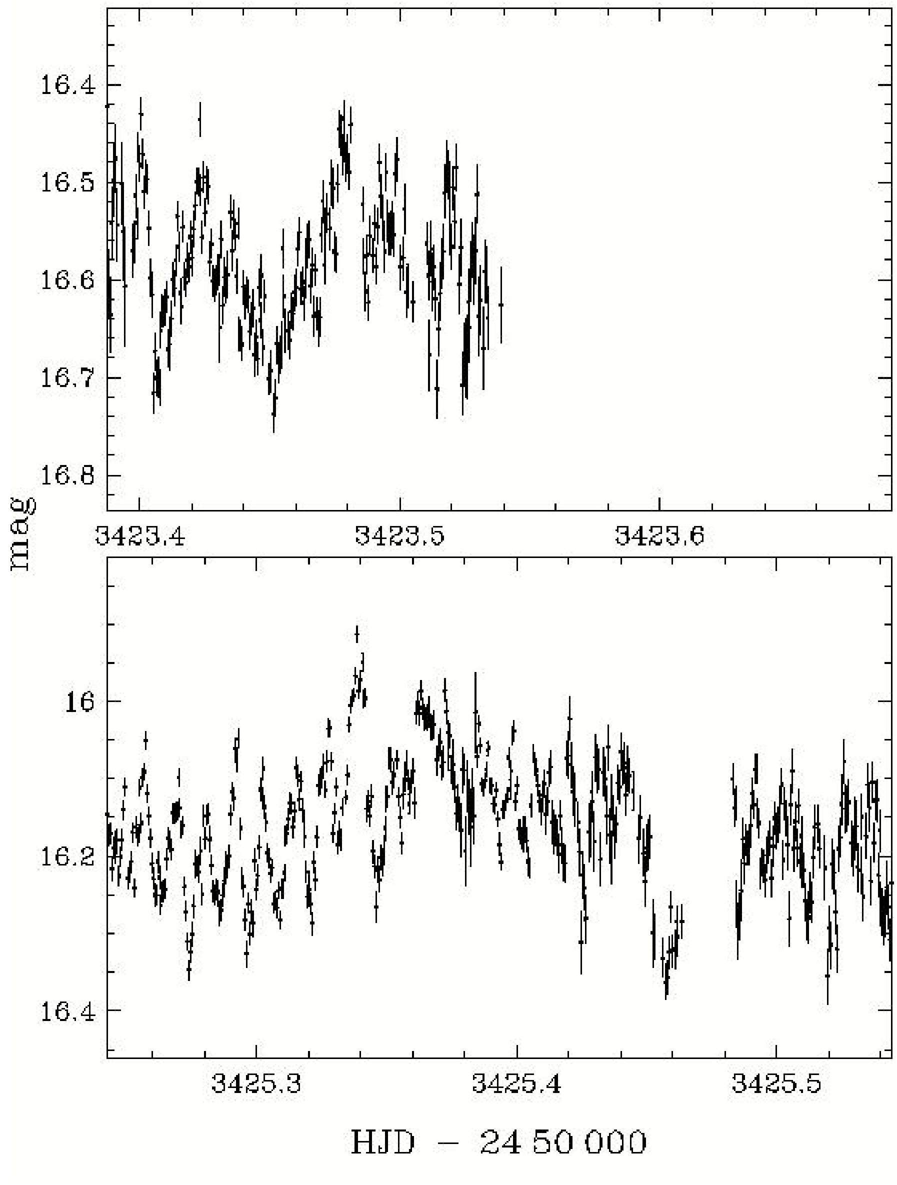

Figure 4.3.4: RXJ0636+3535 lightcurves. Top to bottom: 21/02/2005, 23/02/2005

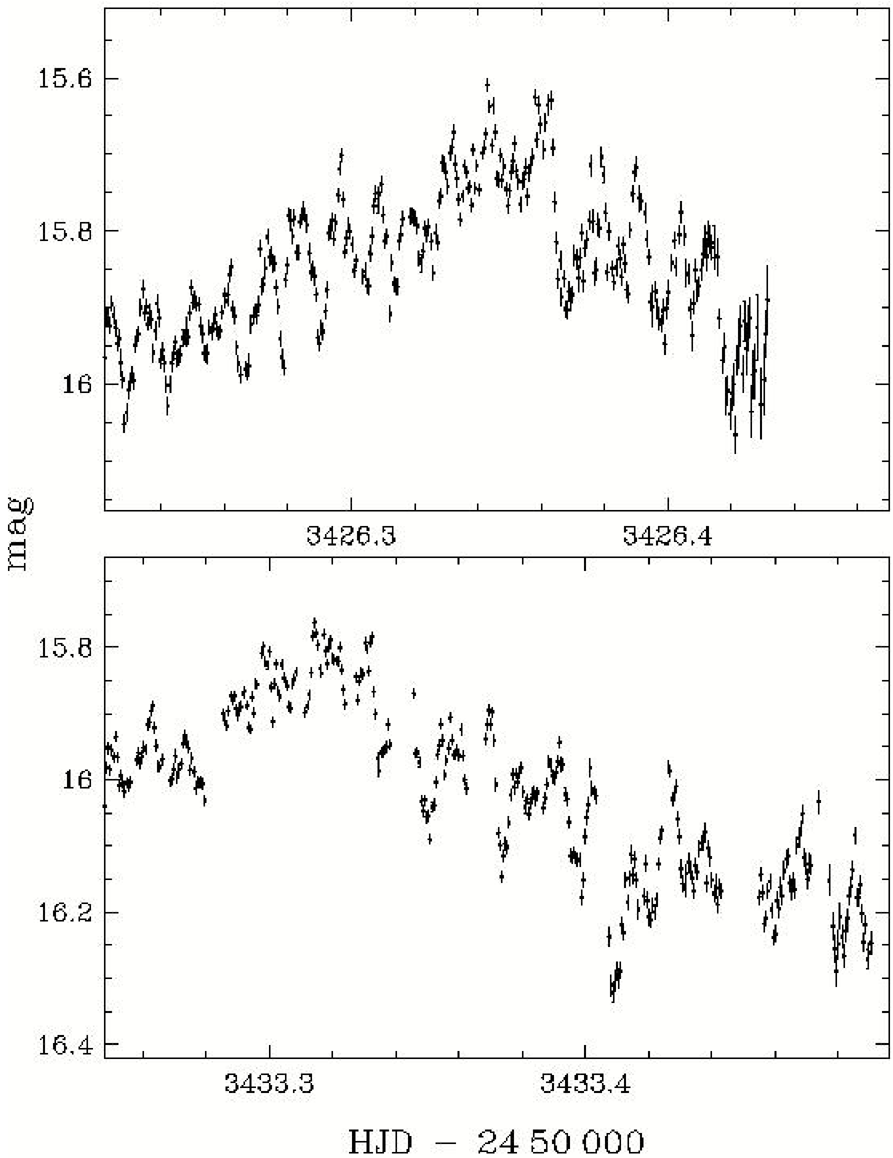

Figure 4.3.5: RXJ0636+3535 lightcurves. Top to bottom: 24/02/2005, 03/03/2005

Chapter 5

Discussion

5.1 Introduction

In this fifth, and final, Chapter of the diploma thesis we will take a closer look to the results of the previous Chapter. We will sumarise what information we got from the lightcurves and try to put it into physical context.

5.2 About HS2325+8205

Regarding HS2325+8205, as it can be clearly seen in Table (4.2.1) both the mirroring and the polynom fit methods produce almost identical eclipse centre timings. This fact makes us confident of the credibility of our calculations.

Based on these eclipse centre timings we believe HS2325+8205 to have an orbital period of

$$P_{\mathrm{orb}} \sim 279.841927 \pm 0.000117 \text{ min} \tag{5.2.1}$$

Furthermore, we have also deduced an ephemeris for the system, which - as mentioned before - is

$$T_0 = 2452888.425254 \pm 0.000247 + E * 0.1943346715 \pm 0.0000000815 \tag{5.2.2}$$

Using this ephemeris an O-C diagram has been calculated and is presented in the Figure (5.2.1).

It can clearly be seen that the last two nights deviate significantly. This is “natural”, in a way, as there is a 605-days gap between the observations (23/10/2004 - 23/08/2006) yielding a loss of about 3113 orbital cycles, so it is uncertain if the orbital cycle on 23/08/2006 is the 3113th or the 3112th one.

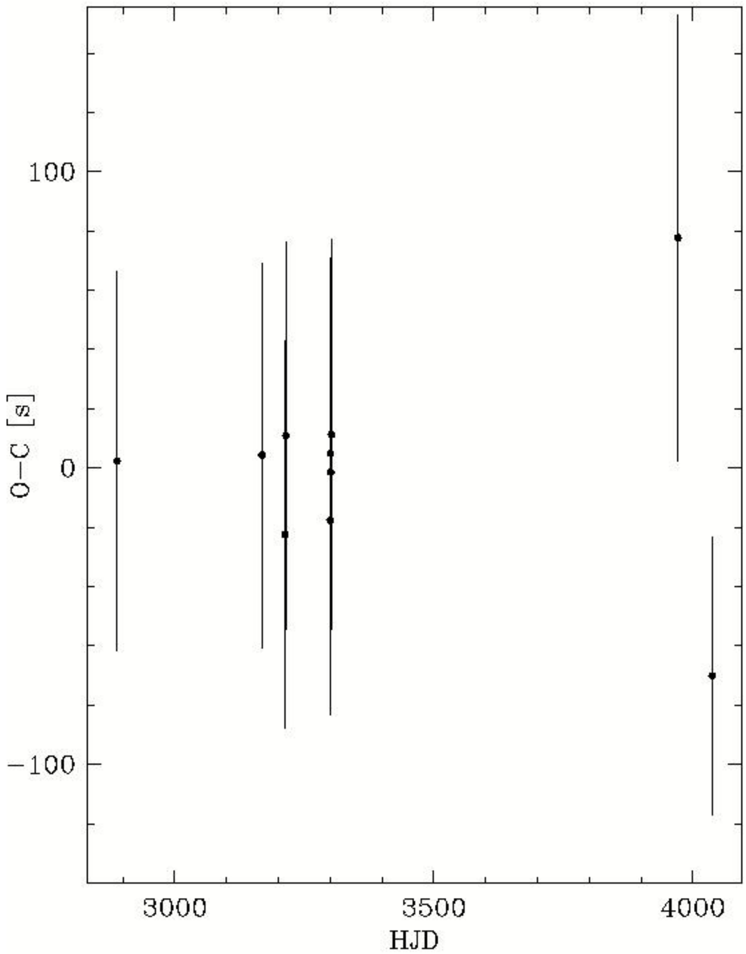

Figure 5.2.1: The O-C diagram of HS2325+8205 using ephemeris 5.2.2

Additional data and observations, either from nights between 2004-2006 or from new runs in 2007 are needed in order to improve the ephemeris and get a more accurate estimate of the orbital period.

The exciting behaviour of HS2325+8205 is fully depicted in the lightcurves of Figure (5.2.2). As we have mentioned in Section (1.7), the eclipse profile depends on the dominant light-emitting feature of the system, be it the white dwarf, the hot spot or the accretion disc (for a better insight on the subject see for example [13], [14], [15] and [16]).

The first lightcurve clearly displays a white dwarf and hot spot dominated lightcurve. The white dwarf ingress starts a bit after 3300,40 and a slight "bump" at about 3300,406 indicates the hot spot ingress. The white

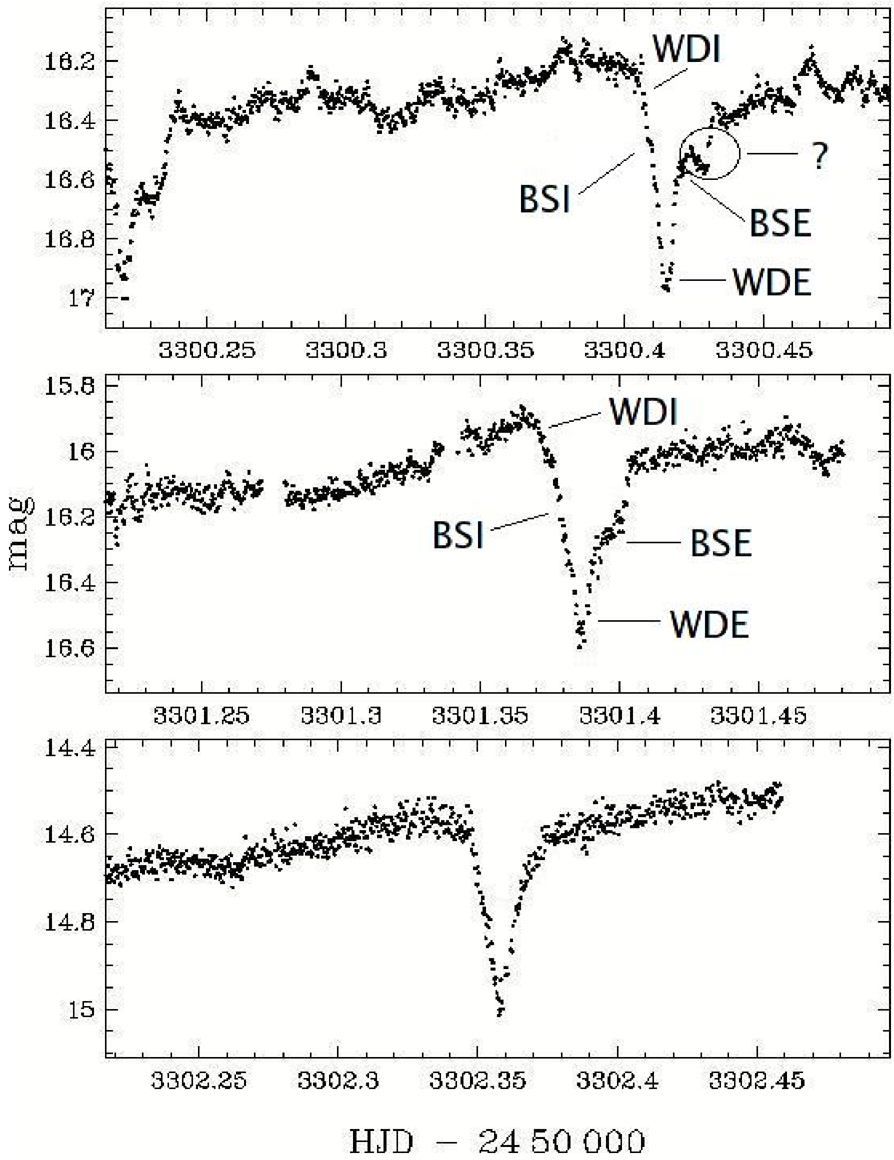

Figure 5.2.2: Analysis of the 21,22,23/10/2004 lightcurves of HS2325+8205

dwarf egress starts at about 3300,415, while the hot spot egress starts at about 3300,42. These features are depicted on the lightcurve, retaining the denotation WDI,WDE,BSI and BSE.

Quite puzzling - and unfortunately with no sufficient explanation - is the structure found immediately after the hotspot egress between 3300,42 and 3300,43, with an eclipse-like feature at 3300,43, noted with a circle and a question mark on the lightcurve.

The third lightcurve - 23/10/2004 - clearly displays a disc dominated eclipse, with quite smooth, almost straight-lined, ingress and egress for the part of the disc being occulted by the red dwarf and with none of the features of the previously described eclipse being detectable.

The second lightcurve - 22/10/2004 - displays an intermediate state of the system. The white dwarf and hot spot ingress and egress can be seen, but this is not the case for the puzzling eclipse structure detected in the first lightcurve.

The parts of the lightcurve before and after the eclipse differ as well, with those from 21/10 displaying significant variations and flickering, while those from 23/10 are almost constant in brightness.

The amazing fact is that these lightcurves are from three consecutive nights! HS2325+8205 is definitely full of surprises as it displays three different profiles in these three nights rrespectively

The difference in the profiles is directly connected to the system's brightness. On 21/10 the eclipse centre is at mag 17, while the eclipse centre on 23/10 is at mag 15. Clearly, when the system is in the "faint" state more *fine* structures and features can be seen, while during its "bright" state the light from the disc washes away everything else. This can also be seen in the "intermediate" state on 22/10, with the eclipse centre at mag 16.6, where only some of the features are visible.

Another quite interesting fact is that HS2325+8205 is rapidly changing magnitude, becoming two magnitudes brighter in two days. It should also be noted that the procedure is not "linear". The eclipse centre goes from mag 17 on 21/10, to mag 16.6 on 22/10, to reach mag 15 on 23/10.

The above described behaviour is in fact characteristic of HS2325+8205, as it can be seen in the other lightcurves as well, for example the one from 27/07/2004 - Figure (4.2.2) - with the system in a deep faint state - eclipse centre at mag 17.6 - with all the features visible, in contrast to the one from 05/09/2003 - Figure (4.2.1) - with the system in a bright state - eclipse centre at mag 15.4 - with none the features visible.

Additional data are required, especially spectroscopic analysis of the accretion disc and estimates of mass transfer rates during the various states of the system, in order to fully understand its behaviour.

Summing up, HS2325+8205 is a perfect example of how complicated CV's can be and also a brilliant proof of how much knowledge of basic astrophysical processes we can obtain by studying these systems.

5.3 About RXJ0636+3535

The lightcurves obtained for RXJ0636+3535 - Figures (4.3.2)-(4.3.5) - display substantial variability on short time-scales (of the order of minutes) superimposed on longer-term variations (of the order of hours).

The suspected presence of a coherent short period modulation is confirmed by the Scargle periodogram - Figure (4.3.1) - with the detection of two strong signal clusters. Table (5.3.1) summarises the results of the periodogram.

Singal	*Freq. peak [d^{-1}]*	*Period [min]*	*Period [s]*
1	85.6852	16.8057	1008.34
2	92.8903	15.5021	930.12

Table 5.3.1: Periodogram results of RXJ0636+3535

Given the magnetic nature of RXJ0636+3535, suggested by its spectroscopic appearance [8], we tentatively interpret these two signals[1] as the white dwarf spin period ω or P_{spin} and the orbital-sideband (beat) frequency $\omega \pm \Omega$ or f_{beat}, with Ω being the orbital period P_{orb} of the system.

The detection of these two signals is the hallmark of *Intermediate Polars*. However, photometric observations alone are not adequate to unambiguously identify the two signals, as both spin and beat dominated IP's are known [7].

Usually in IP's the higher frequency peak is related to the spin and the lower frequency one is related to the beat $\omega - \Omega$. For a better discussion on this subject see [12]. It would possible that the signals are swapped, but this would imply a retrograde motion, for which no IP is known so far.

In any case, if the interpretation of the signals being ω and $\omega \pm \Omega$ is correct, RXJ0636+3535 is expected to have an orbital frequency $\Omega = 7.2051$ cpd yielding an orbital period of

$$P_{\text{orb}} = 199.8584 \pm 0.0002 \text{ min} \tag{5.3.1}$$

RXJ0636+3535 also exhibits an interesting behaviour if one calculates power spectra for each night individually, instead of the all-nights Scargle periodogram of Figure (4.3.1). Table (5.3.2) presents a comparison between the amplitudes of the two signals in every night. The hyphen "-" means that no signal was detected.

[1]The signals in the periodogram are frequencies, however for convenience, we will refer to the respective periods

Based on the data of Table (5.3.2), two distinct kinds of behaviour can be seen in the two observational runs, October 2004 and February-March 2005.

Obs. night	*Ampl. of signal 1*	*Ampl. of signal 2*	*Mean brightness*
20041020	0.02551	-	15.7907
20041021	0.00024	0.00020	15.9331
20041022	0.00050	0.00056	16.3579
20041023	0.04757	-	15.9588
20050221	0.00103	0.00047	16.5805
20050223	0.04256	0.02357	16.1607
20050224	0.03286	0.01773	15.8457
20050303	0.03940	0.01211	16.0196

Table 5.3.2: Comparison of the amplitude of the signals detected in the periodograms from each night of observations of RXJ0636+3535

In the 2004 run, when the lower frequency signal (= signal 1) is strong the higher frequency signal (= signal 2) is not seen. When the former is weak, the latter is at similar intensity.

In the 2005 run both signals are present with the low frequency signal peaking at about twice the intensity of the high frequency one.

The interpretation of Table (5.3.2) is not an easy job. Supposing that signal 1 is the beat frequency, while signal 2 is the white dwarf spin pulsations, this behaviour might imply that RXJ0636+3535 is accreting in an "hybrid" mode - both through disc and through disc-overflow (see Section 1.6.1) - with major accretion via the stream.

However, since the proportion of the one amplitude over the other appears to change with time, it might be that in the 2004 run there are changes in the relative proportion of the two accretion modes. This could be attributed to sudden changes of the mass transfer rate from the secondary star, but there is no data to support the argument. In the 2005 run the stronger amplitude of the beat frequency signal might indicate that the dominant accretion mode is still from the stream [30].

Table (4.3.2) also shows the mean system brightness derived from the lightcurves, which is useful to know, because when changes of amplitudes are observed, these are accompanied by changes (though small) of brightness level, which is indeed the case here.

UUnfortunately the orbital period is poorly covered in these eight nights and as a result one cannot check the amplitude of the orbital signal and whether it has changed over time. This is important because when a beat modulation is present, there is also an orbital variability. In many IP's, where amplitude changes are observed and interpreted as changes of the accretion mode, the orbital modulation also accompanies these changes.

One should also keep in mind that we are dealing with optical data and not with X-ray ones, which would be better to diagnose the true accretion mode (for more information see for example [9], [10] and [11]).

Undoubtedly, further optical data together with additional data from other wavebands as well as time-resolved spectroscopy could help clarify things.

To sum up, based on all the facts, we believe RXJ0636+3535 to be an Intermediate Polar with an orbital period of $P_{\rm orb} = 199.8584 \pm 0.0002$ min and a white dwarf spin period of either $P_{\rm spin} = 16.8057 \pm 0.0001$ min or $P_{\rm spin} = 15.5021 \pm 0.0002$ min.

5.4 Conclusions

The goal of this Diploma Thesis was to observe, analyse the gathered data and investigate the periodicities of Cataclysmic Variable stars, using modern astronomical techniques. We have seen how each system's characteristic signature, ie its lightcurve, can provide a wealth of usefull information about it and also means to extract this information.

For a quicker reference, we would like to sum up our results one more time. We believe (i) HS2325+8205 to have an orbital period of $P_{\rm orb} \sim 279.841927 \pm 0.000117$ min and the following ephemeris $T_0 = 2452888.425254 \pm 0.000247 + E * 0.1943346715 \pm 0.0000000815$ and (ii) RXJ0636+3535 to be an Intermediate Polar with an orbital period of $P_{\rm orb} = 199.8584 \pm 0.0002$ min and a white dwarf spin period of either $P_{\rm spin} = 16.8057 \pm 0.0001$ min or $P_{\rm spin} = 15.5021 \pm 0.0002$ min.

Bibliography

BOOKS

In English

[1] C.Hellier, *Cataclysmic Variable Stars*, Springer Verlag - Praxis, ISBN 1-85233-211-5

[2] J.Frank, A.King, D.Raine, *Accretion Power in Astrophysics*, Cambridge University Press, ISBN 0-521-62957-8

[3] B.W.Carroll, D.A.Ostlie, *An Introduction to Modern Astrophysics*, Addison-Wesley Publishing Company Inc., ISBN 0-201-54730-9

In Greek

[4] H.Varvoglis, J.H.Seiradakis, *Introduction to Modern Astronomy*, Gartaganis Publications, ISBN 960-7013-21-2

[5] S.Avgoloupis, J.H.Seiradakis, *Observational Astronomy*, Aristotle University of Thessaloniki Publications, 1993

[6] N.Spyrou, *Principals of Stellar Evolution*, Paratiritis Publications, 2003

PAPERS

[7] S.Pyrzas et al, *RXJ0636+3535 - A new intermediate polar*, 2006AIPC..848..432P

[8] B.T.Gänsicke et al, *Cataclysmic variables from a ROSAT/2MASS selection - I.Four new intermediate polars*, 2005MNRAS.361..141G

[9] T.L.Parker, A.J.Norton, K.Mukai, *X-ray orbital modulations in intermediate polars*, 2005A&A...439..213P

[10] P.A.Evans, C.Hellier, HT Camelopardalis: the simplest intermediate polar spin pulse, 2005MNRAS.359.1531E

[11] C.Hellier, *The accretion geometry of intermediate polars*, 1995ASPC...85..185H

[12] B.Warner, *Multiple orbital sidebands in intermediate polars*, 1986MNRAS.219..347W

[13] W.J.Feline et al, *ULTRACAM photometry of the eclipsing cataclysmic variable OU Vir*, 2004MNRAS.355....1F

[14] J.H.Wood et al, *Eclipse studies of the dwarf nova OY Carinae in quiescence*, 1989ApJ...341..974W

[15] J.H.Wood et al, *High-speed photometry of the dwarf nova Z Cha in quiescence*, 1986MNRAS.219..629W

[16] J.H.Wood, M.J.Irwin, J.E.Pringle, *A digital technique for the separation of the eclipses of a white dwarf and an accretion disc*, 1985MNRAS.214..475W

[17] W.Voges et al, *The ROSAT all-sky survey bright source catalogue*, 1999A&A...349..389V

[18] H.J.Hagen et al, *The Hamburg Quasar Survey. I. Schmidt observations and plate digitization*, 1995A&AS..111..195H

[19] B.T.Gänsicke et al, *HS 2237+8154: On the onset of mass transfer or entering the period gap?*, 2004A&A...418..265G

[20] E.Bertin, S.Arnouts, *SExtractor: Software for source extraction*, 1996A&AS..117..393B

[21] J.D.Scargle, *Studies in astronomical time series analysis. II - Statistical aspects of spectral analysis of unevenly spaced data*, 1982ApJ...263..835S

[22] J.E.Pringle , *Accretion discs in astrophysics*, 1981ARA&A..19..137P

[23] D.Lynden-Bell, J.E.Pringle, *The evolution of viscous discs and the origin of the nebular variables*, 1974MNRAS.168..603L

[24] N.I.Shakura, R.A.Sunyaev, *Black holes in binary systems. Observational appearance*, 1973A&A....24..337S

WEBSITES

[25] http://www.astro.noa.gr/ASK_1.2m/ask_main.htm

[26] http://www.eso.org/projects/esomidas/

[27] http://spiff.rit.edu/match/

[28] http://www.astro.princeton.edu/~rhl/sm/

[29] http://deneb.astro.warwick.ac.uk/phsdaj/public_html/Software/Period/

OTHER

[30] Domitilla de Martino, *personal contact*